21st ANNUAL CONFERENCE OF INDIAN RADIOLOGICAL & IMAGING ASSOCIATION

JHARKHAND CHAPTER

7TH APRIL, 2024

RAJENDRA INSTITUTE OF MEDICAL SCIENCES, RANCHI

THEME : "REVOLUTIONIZING RADIOLOGY: EXPLORING IMAGERY BEYONG BOUNDARIES"

SOUVENIR



FUJIFILM
Value from Innovation

Introducing

FUJIFILMS EXPANDED PORTFOLIO

OF HEALTHCARE SOLUTIONS

MAMMOGRAPHY &
BONE DENSITOMETRY

MRI

MOBILE X-RAY

IVD

ULTRASOUND

X-RAY

CT

PORTABLE X-RAY

VNA
PACS
3D
SYNAPSE®
Enterprise Imaging
Mobility
AI
RIS

Fujifilm India Pvt Ltd

Unitech Cyber Park Unit No. 801-807, 8th Floor, Tower C,
Sector 39, Gurugram - 122001, Haryana | Tel : +91-(0)124-4325400

21st ANNUAL CONFERENCE OF
INDIAN RADIOLOGICAL & IMAGING ASSOCIATION
JHARKHAND CHAPTER

7TH APRIL, 2024
RAJENDRA INSTITUTE OF MEDICAL SCIENCES, RANCHI

THEME : "REVOLUTIONIZING RADIOLOGY: EXPLORING IMAGERY BEYONG BOUNDARIES"

SOUVENIR

SPONSORS


FUJIFILM


BAYER


Allengers
Passion for excellence


SAMSUNG


mindray


SIEMENS
Healthineers


PHILIPS


JB


DOCLAND
SYMBOL OF DEDICATION AND PERFECT PROTECTION


Manipal
HealthMap


mjm
you think it we ink it...

Organizing Committee

Patron in chief
Dr Chandra Mohan

Patron:
Dr OPN Choudhary

Patron
Dr. OK Singh

Organizing Chairman
Dr Prof. S. K Toppo

Organizing Secretary
Dr Rajeev K Ranjan

Organizing Co-Chairman
Dr P. Sen

Treasurer
Dr Sangita Jha

Joint Secretary
Dr Anish Choudhary

Conference Co-Ordinator
Dr K. A Rajan Pandey

Organizing Committee


Dr. Manoj Kumar Singh


Dr. Zia ur Rahman


Dr. Manish Kumar


Dr Chitraranjan


Dr. Pravin Tripathy


Dr. Shekhar Sharma


Dr. J P Pal


Dr. Dr. Madhu Sharma


Dr Mukta Agarwal


Dr. KS Mahan


Dr. Nlsha Rai


Dr. Anima Xalxo


Dr. Vijay Kr. Agarwal


Dr Shwetam kumar


Dr. Amlt Kr. Singh


Dr. Ajft Kumar


Dr. Pumima Deam


Dr. Nishikant


Dr. Ambuj srivastav


Dr Ishteyaq

IRIA State Office Bearers

Past President
Dr Chandra Mohan

President
Dr Niraj Kumar

President Elect
Dr. JK Singh

Vice-President
Dr Sushmlta Renu

Vice-President
Dr M K Bhadani

Treasurer
Dr Rajeev K Ranjan

Secretary
Dr Probal Sen

Jt.Secretary
Dr AK Barnwal

Jt. Secretary
Dr. Shailendra Choudhary

Member Central Council
Dr Manish Kumar

Member Central Council
Dr P. K Purbay

Member State Council
Dr Amit Kr. Singh

Member State Council
Dr Pramod Kumar

Vivere IMAGING

INVESTED IN SCIENCE

More than 4'00'000 Scans in India

US FDA REGISTERED API

ASSURED QUALITY

Vivhexol 350

℞ Iohexol Injection USP 350 mg I/mL

Non-ionic contrast medium in sterile aqueous solution

Solution for injection

50 mL

100 mL

with Wide Range of Indications

Approved in all age groups including Neonates

Low-osmolar | Non-Ionic

India's Leading 1 Molar MRI - Contrast Agent

VIV-BUTROL

Gadobutrol Injection

1 Molar macrocyclic

VIVIDSCAN

Macrocyclic MRI Contrast Agent

MEGLUMINE GADOTERATE

(Gadoteric Acid)

0.5 Molar - Macrocyclic

GADOBRIGHT

Gadopentetate Dimeglumine USP

0.5 Molar MRI Contrast Agent for enhanced image

बन्ना गुप्ता
मंत्री

झारखण्ड सरकार
GOVERNMENT OF JHARKHAND

स्वास्थ, चिकित्सा शिक्षा एवं परिवार कल्याण
तथा आपदा प्रबंधन विभाग
नेपाल हाउस, डोरण्डा, राँची-834002
फोन : 0651-2482492/2482493
ई-मेल : hm.jharkhand@gmail.com

MESSAGE

It gives me immense pleasure to extend my warmest greetings to all participants of the 21st Annual IRIA Jharkhand Chapter Conference, to be held at RIMS Ranchi on April 7th, 2024.

The Jharkhand State Radiologists' Conference (JSRC) has been a cornerstone event in our calendar, fostering collaboration, innovation, and excellence in the field of radiology.

Radiology plays a pivotal role in modern healthcare, enabling accurate diagnoses and guiding effective treatments. As we navigate through the challenges of healthcare delivery, particularly in the wake of the ongoing global health crisis, the role of radiologists becomes increasingly crucial.

I encourage all participants to actively engage in the conference proceedings, share knowledge, and explore new avenues for collaboration. I aspire that this platform may be used to exchange ideas, learn from each other's experiences, and collectively strive towards enhancing healthcare delivery especially in Jharkhand.

I extend my gratitude to the organizers, sponsors, and participants for their unwavering commitment to advancing the field of radiology in Jharkhand.

Wishing you all a successful and enriching conference.

Warm regards,

(Banna Gupta)

राजेन्द्र आयुविज्ञान संस्थान
(झारखण्ड सरकार का एक स्वायतशासी संस्थान)
राँची-834009 (झारखण्ड)
दूरभाष : 0651-2541533 फैक्स : 0651-2540629,
ई-मेल : rimsranchi@rediffmail.com

RAJENDRA INSTITUTE OF MEDICAL SCIENCE
(An Autonomous Institute under Govt. of Jharkhand)
Ranch--834009 (Jharkhand)
Phone : 0651-2541533, Fax : 0651-2540629
Email : rimsranchi@rediffmail.com

MESSAGE

It is a matter of great pleasure for me to forward a message on the occasion of 21st annual conference of Indian Radiological and Imaging Association, Jharkhand chapter being organised in Rajendra Institute of medical sciences, Ranchi on 7 April 2024.

On this occasion, I greet the members and delegates and welcome them to the land of Bhagwan Birsa Munda to disseminate knowledge and skill among young professionals, seasoned practitioners and researcher. My good wishes for the Conference and release of souvenir.

(Prof. Dr. Rajkumar)
Director
Rajendra Institute of Medical Sciences,
Ranchi

Greetings to All at JSRC2024

MESSAGE

Dear Colleagues,

At the outset, I would like to congratulate the Jharkhand state chapter of Indian Radiological & Imaging Association for organizing its 21st Annual Conference (JSRC2024), which is scheduled to be held at RIMS Ranchi on April 7th, 2024. It is my proud privilege to be associated with this conference.

The deliberations at this conference will definitely enhance the knowledge, skills and expertise of the participants on the latest advancement in Radiology and Imaging and help in developing strategies in monitoring performance of medical systems for the betterment of mankind. The aim of our association is to promote the study and practice of Radio-diagnosis & Imaging and it can be achieved by conducting more and more academic programs like Conferences, CMEs, Seminars, Workshops, Symposia etc.

I wish high quality scientific deliberations by eminent speakers will serve a great academic feast to the residents and young radiologists. I hope the Organizing Committee under the leadership of Prof. Dr. S K. Toppo, Organizing Chairman along with Dr. Rajeev K. Ranjan, Organizing Secretary; Dr. Probal Sen, Organizing Co-Chairman; Dr. Anish Choudhary, Organizing Joint Secretary and their entire team will leave no stone unturned to make this conference successful.

I once again congratulate you all for holding this great state annual meeting.

Long Live IRIA!!

JAI HIND!

(Dr. V.N. Varaprasad)
President, IRIA

A Heartfelt Welcome to the 21st Annual Conference of the IRIA Jharkhand Chapter

MESSAGE

Esteemed Radiologists, Distinguished Guests, and Dear Friends,

As the President of the Indian Radiological and Imaging Association state chapter, it is my profound honour' to welcome you to the 21st Annual Conference of the IRIA Jharkhand Chapter, JSRC2024, to be held at the prestigious RIMS Ranchi Academic Block on April 7th, 2024.

This gathering is not just a conference; it is a celebration of our relentless pursuit of excellence in the field of radiology. The Souvenir magazine will encapsulate our shared experiences, the knowledge disseminated, and the innovative ideas that will emerge from our collective wisdom.

I am filled with pride as we stand on the cusp of another milestone event that promises to shape the future of radiology in India. Let us come together to make JSRC2024 a symposium of learning, a confluence of ideas, and a beacon of inspiration for radiologists everywhere.

I eagerly await the opportunity to meet and engage with you all. Until then, may we continue to strive for the betterment of our profession and the health of our society.

With warmest regards,

Dr, Niraj Kumar
President, IRIA, Jharkhand State

A Warm Welcome to JSRC2024

MESSAGE

Dear Colleagues and Esteemed Guests,

It is with great honour and excitement that I extend a heartfelt welcome to each one of you to the 21st Annual Conference of the IRIA Jharkhand Chapter, JSRC2024, scheduled to take place on April 7th, 2024, at the RIMS Ranchi Academic Block.

As we convene under the theme 'Radiology: Reflecting the Spectrum of Life', we stand united in our passion for the field of radiology and our commitment to the betterment of patient care through innovation and education.

The Souvenir magazine will capture the essence of our gathering, highlighting the advancements, the camaraderie, and the shared knowledge that this conference will undoubtedly foster. It will serve as a cherished keepsake that commemorates our collective efforts and the strides we are making in radiology.

I am confident that the JSRC2024 will be a landmark event, filled with enriching experiences, engaging discussions, and opportunities for professional growth. Let us look forward to an inspiring conference that will propel us forward in our endeavours.

Once again, welcome to JSRC2024. Together, let's make this conference a memorable and transformative experience.

With warm regards,

Suresh

Dr. Suresh Kumar Toppo
Chairperson, JSRC2024

Welcome all delegates to the 21st Annual Conference of the IRIA Jharkhand Chapter - JSRC2024

MESSAGE

On behalf of the organizing committee, it is my immense pleasure to welcome all the esteemed delegates, revered members, and distinguished guests to the JSRC2024, held at the RIMS Ranchi Academic Block on the 7th of April, 2024.

As we gather in the vibrant city of Ranchi, we are reminded of the rich heritage and the collaborative spirit that the Indian Radiological and Imaging Association (IRIA) embodies.

We are thrilled to present a program brimming with insightful lectures, interactive sessions, and groundbreaking research presentations that promise to enrich our knowledge and sharpen our skills. The Souvenir magazine, a memento of our journey, will encapsulate the essence of this conference, preserving the memories and milestones we achieve together.

Let us embrace this opportunity to learn, network, and inspire each other towards greater heights in the field of radiology. Welcome to JSRC2024, where minds meet and visions converge.

Warm regards

Dr. Rajeev Kumar Ranjan
Organizing Secretary,
JSRC2024

Greetings to All at JSRC2024

MESSAGE

As the secretary of the IRIA Jharkhand Chapter, it is my privilege to welcome you to the 21st Annual Conference, JSRC2024, taking place on the 7th of April, 2024, at the RIMS Ranchi Academic Block.

This year, we are excited to bring together the brightest minds in radiology, offering a platform for professional exchange and innovation. The Souvenir magazine will serve as a chronicle of our shared experiences and a showcase of the pioneering work that continues to drive our field forward.

We look forward to the knowledge that will be shared, the relationships that will be formed, and the future that we will shape together at this conference. May the Souvenir magazine be a testament to the spirit of collaboration and advancement that defines our chapter.

Welcome to a day of learning, inspiration, and camaraderie. Welcome to JSRC2024.

With warmest regards,

Dr. Probal Sen
Co-chairpesron, JSRC2024

GE HealthCare

3 Decades of Innovation

LOGIQ™ Redefined

General Imaging Range of Solutions

Powerful enough to handle limitless applications

LOGIQ™ E10s R3

LOGIQ™ Fortis

LOGIQ™ P10 XD Clear

LOGIQ™ P9 XD Clear

LOGIQ™ P8

Liver Fat & Fibrosis Quantification

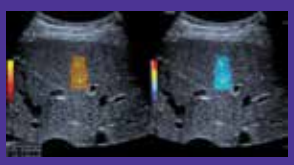

2D Shear Wave Elastography

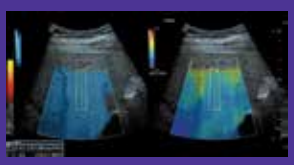

UGAP-Ultrasound Guided Attenuation Parameter

3D/4D Imaging

Color Radiant*flow* imaging

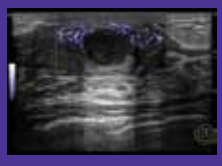

Highly detailed image to detect and characterize breast disease

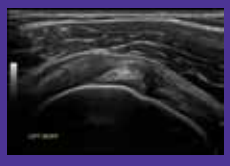

Excellent details and contrast resolution for musculoskeletal conditions

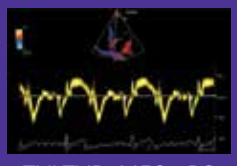

TVI TVD, M5Sc-RS

www.gehealthcare.in | Toll-free Number :1800-102-2977

Contact: **Somnath, +91 98532 05159**

IRIA Members

S.No.	NAME	RESIDENCE	FOLIO NUMBER	CONTACT NUMBER
1	A R KAZMI	GIRIDIH	1EM/JH-7	NA
2	R N RAY	BOKARO	2EM/JH-6	9430771264
3	RAM NARAYAN VERMA	RAIPUR	1LM/2H-1	7898337590
4	KASHINATH SHARMA	JAMSHEDPUR	5LM/JH-2A	0657-2226550
5	MADHUP LAL	RANCHI	6LM/JH-2B	NA
6	ABHIJIT SARKAR	DHANBAD	10LM/JH-4	NA
7	SUJIT KUMAR PAL	RANCHI	14LM/JH-5A	NA
8	DEVESH BAHADUR	JAMSHEDPUR	15LM/JH-5B	NA
9	SURYA KUMAR BASU	RANCHI	18LM/JH-6B	9431101377
10	SUBHASH CHANDRA BOSE	DHANBAD	22LM/JH-8	9431169068
11	JITENDRA KUMAR SINGH	RANCHI	23LM/JH-8A	NA
12	ARUN KUMAR VERMA	JAMSHEDPUR	26LM/JH-9A	0657-2360460
13	JUDHAJIT P PAL	RANCHI	27LM/JH-9B	0651-2462653
14	RAJEEV KUMAR RANJAN	PATNA	31LM/JH-11A	0612-274036
15	SANGITA JHA	PATNA	32LM/JH-11B	0612-523259
16	SURESH KUMAR TOPPO	RANCHI	33LM/JH-12A	9430372656
17	MADHU SHARMA	RANCHI	34LM/JH-12B	9835143617
18	PROBAL SEN	RANCHI	38LM/JH-14	9835193047
19	DIVYASHREE	HALDWANI	39LM/JH-14B	9368544799
20	JAWAHAR DUTTA	DHANBAD	40LM/JH-15	9720738969
21	SANDEEP J	DHANBAD	41LM/JH-15A	NA
22	MUKTA AGRAWAL	RANCHI	43LM/JH-16	9471605549
23	RAKESH KUMAR VIDROHI	RANCHI	46LM/JH-17	9386608299
24	VIPIN KUMAR PATHAK	NAVI MUMBAI	47LM/JH-17A	9934943430
25	VOILET MURMU	JAMSHEDPUR	49LM/JH-18	9525113777
26	SUNITA KUMARI	WEST BENGAL	50LM/JH-18A	9547134747

S.No.	NAME	RESIDENCE	FOLIO NUMBER	CONTACT NUMBER
27	PUNAM BARA	RANCHI	51LM/JH-18B	9934321671
28	PUJA BHAGAT	JAMSHEDPUR	53LM/JH-19	9430747579
29	SUBODH BAGE	JHUMRI TALAIYA	54LM/JH-20	8986684331
30	SULTAN ALI SAIFULLAH	JAMSHEDPUR	56LM/JH-20B	9430388073
31	SIDDHARTH SINHA	JHARKHAND	57LM/JH-191	NA
32	ANIL KUMAR GUPTA	JAMSHEDPUR	58LM/JH-191A	9431117305
33	NEETU KUMARI	JAMSHEDPUR	59LM/JH-191B	9430731805
34	SUSMITA RENU	JAMSHEDPUR	60LM/JH-192	9708601448
35	SUDHA JHINGON	JAMSHEDPUR	61LM/JH-193	9102404801
36	VARSHA MARY KHALKHO	JAMSHEDPUR	62LM/JH-193A	8056923475
37	KUSHAL SINGH	JAMSHEDPUR	63LM/JH-193B	7368806285
38	SOURAV PANDA	BHUBANESHWAR	64LM/JH-194	9031150537
39	MANISH KUMAR LALL	DEOGHAR	65LM/JH-194A	9431521220
40	MANOJ KUMAR JHA	DEOGHAR	66LM/JH-194B	7631059838
41	KUMARI MADHULATA	B. DEOGHAR	67LM/JH-195	9162160583
42	SHAILENDRA K. CHOUDHARY	DIST- GIRIDIH	68LM/JH-195A	9934390975
43	RITIKA THAKUR	RANCHI	69LM/JH-195B	9234611372
44	JYOTI SUSHMA DADEL	JAMSHEDPUR	70LM/JH-196	9031080150
45	DEEPAK KUMAR	JAMSHEDPUR	71LM/JH-196A	9431186857
46	RAJEEV KUMAR BISWAS	DURGAPUR	73LM/JH-199	9233368411
47	KAPIL AGGARWAL	BOKARO STEEL CITY	75LM/JH-19A	9798180544
48	SANJAY KUMAR	DHANBAD	77LM/JH-208	9204424168
49	TANUSHRI GHOSH	RANCHI	78LM/JH-192A	8789319644

ARTICLES

A Correlational Study of Ophthalmic Artery Doppler Parameters and Maternal Blood Pressure in Normotensive and Pre-eclamptic Pregnancies at a Tertiary Care Hospital

Neha Kumari,[1] Rajeev Kumar Ranjan,[1] Nisha Rai,[1] Anima R Xalxo, Suresh K Toppo,[1] and Paras Nath Ram[1]

Abstract

Background

Hypertensive disorders are one of the most common complications of pregnancy. This study aimed to investigate the relationship between ophthalmic artery Doppler indices and preeclampsia development and evaluate differences in these indices between normotensive and hypertensive pregnancies.

Methods

A hospital-based cross-sectional observational study was conducted involving a sample size of 80 pregnant women: 40 normotensive and 40 preeclamptic. The participants' ophthalmic artery Doppler parameters were evaluated using ultrasonography. Various clinical and demographic factors were also collected for analysis.

Results

Significant differences in the pulsatility index (PI) and end-diastolic volume (EDV) of the ophthalmic arteries were found between the normotensive and preeclamptic participants ($p < 0.05$). An inverse correlation was observed between the ophthalmic artery PI (OAPI) and mean maternal arterial pressure, suggesting reduced orbital vascular resistance and increased orbital flow. Moreover, the decrease in PI was more significant in severely preeclamptic women than in mildly preeclamptic and normotensive women. The findings indicated a significant correlation between ophthalmic artery Doppler parameters and the development of preeclampsia. The decrease in OAPI was particularly profound in women with severe preeclampsia. However, the study was limited by its small sample size and the lack of matching of participants based on maternal age, gestational age, and other factors.

Conclusions

The study results suggest that ophthalmic artery Doppler parameters, mainly PI and EDV, could serve as reliable indicators for the development of preeclampsia. Given their safety, cost-effectiveness, and accessibility, these parameters can help differentiate between preeclamptic and normotensive pregnancies in late gestation. Further research with larger sample sizes and matched participant groups is recommended for more conclusive results.

Introduction

Hypertensive disorders represent one of the prevalent pregnancy complications, affecting 7% to 15% of patients [1]. These disorders correlate with high maternal and perinatal morbidity and mortality [2]. Moreover, they are strongly linked with fetal growth restriction, low birth weight, spontaneous or iatrogenic preterm delivery in approximately 8% to 10% of cases [3], respiratory distress syndrome, admission to neonatal intensive care, and cerebral palsy [4]. The categorization of hypertensive disorders during pregnancy includes four distinct groups: gestational hypertension, preeclampsia, eclampsia, chronic hypertension (essential, secondary), and preeclampsia superimposed on chronic hypertension. In primigravidas, hypertensive disorders cause preterm delivery in 0.3% of cases (approximately one in 250) [3]. Placental disorders, such as preeclampsia, result in less than the 10th percentile of birth weight for gestation in 20% to 25% of preterm births and 13% to 19% of term births [3].

According to hemodynamic studies, generalized arteriolar vasoconstriction in preeclampsia results in hypoperfusion of the targeted organs, disruption of the blood-brain barrier, and failure of cerebral autoregulation. This failure causes cerebral vasculature, including the ophthalmic arteries, to be

overperfused. The association between ophthalmic artery Doppler indices and preeclampsia does not appear to result from trophoblast invasion but may relate to maternal hemodynamic adaptation during pregnancy [5]. As a result, color Doppler has been used to visualize and measure flow in retrobulbar blood vessels [6]. Ophthalmic artery Doppler assessments performed between 35 and 37 weeks gestation can predict the subsequent onset of preeclampsia [7].

The ophthalmic artery presents an accessible opportunity to monitor maternal cardiovascular changes, particularly in hypertensive disorders of pregnancy. With functional, embryological [8], and anatomical similarities to intracranial vessels [9,10], the ophthalmic artery can provide insights into the small-caliber intracerebral vasculature and its hemodynamics that are challenging to image transcranially [9].

While magnetic resonance imaging safely allows the study of intracranial blood flow during pregnancy, it is expensive, not readily available, and contraindicated for patients with ferromagnetic implants. Other radiological imaging modalities for assessing the intracranial blood vessels, such as catheter angiography, computed tomographic angiography, and radionuclide imaging, use ionizing radiations. Hence, these modalities pose hazards to the fetus and are contraindicated in pregnancy [11]. Transcranial Doppler ultrasound is a safe and fast method to study intracranial vessels, yet it is challenging to use, offers poor spatial resolution, and requires significant technical expertise for accuracy [11]. Additionally, transcranial Doppler imaging equipment is often unavailable in many low-income nations.

Conversely, ophthalmic artery Doppler is cost-effective, accurate, repeatable, noninvasive, and objective without ionizing radiation exposure. Inspecting the ophthalmic artery is technically feasible as eyeballs lack bone, fat, or gas structures. This technique also boasts a predictive value for developing early onset preeclampsia, similar to uterine artery Doppler evaluation [5].

This study aimed to investigate potential differences in ophthalmic artery Doppler parameters between normotensive and hypertensive pregnancies and establish a correlation between ophthalmic artery pulsatility index (OAPI) and maternal blood pressure (BP).

Materials and methods

We conducted this hospital-based cross-sectional study in the Radiology Department at Rajendra Institute of Medical Sciences (RIMS), Ranchi, Jharkhand, India, from January 2021 to November 2022. We completed a thorough literature survey over one year before we collected the sample, which fell within the study period. The Institutional Ethical Committee of RIMS provided ethical approval (Approval no. 62/IEC/RIMS, dated 17/05/2022). All participating patients gave their informed consent.

The study population included 80 pregnant women: 40 normotensive and 40 preeclamptic, all referred to the Department of Radiology for fetal well-being assessment. The sample size stemmed from a survey by Hata et al. [12]. We selected participants from various gestational periods.

Inclusion criteria for preeclamptic pregnant women required a gestational age over 20 weeks, BP equal to or above 140/90 mmHg, and proteinuria exceeding 0.3 g/l in a 24-hour urine sample or at least a 2+ on a dipstick random urine test. Severe preeclampsia required a gestational age of over 20 weeks with a sustained BP equal to or above 160/110 mmHg. We excluded women diagnosed with diabetes, those on corticosteroids, individuals with a history of addiction, ocular disease, vasculitis, or other vascular diseases, or those who did not provide consent.

We collected data, including the patient's name, age, occupation, and socio-economic status. We also took a detailed clinical history, noting presenting concerns such as headache, ankle swelling, disturbed sleep, blurred vision, or decreased urinary output. We gathered comprehensive obstetric records, noting gravida, parity, similar episodes in previous pregnancies, and medical history of hypertension or diabetes. We measured BP in the brachial artery, using the fourth Korotkoff sound to determine the diastolic pressure. We examined all pregnant women for urinary proteinuria via dipstick and 24-hour routine urine and graded them accordingly.

We placed patients supine during the ultrasound examination, applying the gel directly on the closed eyelid and instructing them to keep the eyeball

fixed and move as directed (Figure (Figure1).1). We examined both ophthalmic arteries within the orbit, starting with the right (Figure (Figure2).2). We kept the angle of insonation below 20 degrees and set the Doppler sample volume to 2 mm. We identified the ophthalmic artery on the medial side of the optic nerve using color Doppler flow imaging and measured the flow velocity approximately 15 mm from the optic disc.

Figure 1

Probe position for ophthalmic artery study.

Figure 2

Ophthalmic artery in colour Doppler

We avoided excessive eyelid compression with the transducer during the examination. We averaged the maternal ophthalmic artery peak systolic velocity (PSV), end-diastolic velocity (EDV), time-averaged mean peak velocities, and pulsatility index (PI) for each side (Figure (Figure3).3). We evaluated the mean PI for statistical analysis by averaging the values obtained from the right and left sides. We measured PI, resistive index (RI), PSV, and EDV using pulsed Doppler ultrasonography with a 6- to 13-MHz linear transducer and a 1- to 5-MHz sectoral probe transducer in a Sonosite ultrasonography machine (Fujifilm Sonosite, Bothell, WA, USA). We calculated gestational age in weeks using ultrasonography per Hadlock [13] considering parameters such as crown-rump length, biparietal diameter, head circumference, abdominal circumference, and femur length.

Figure 3

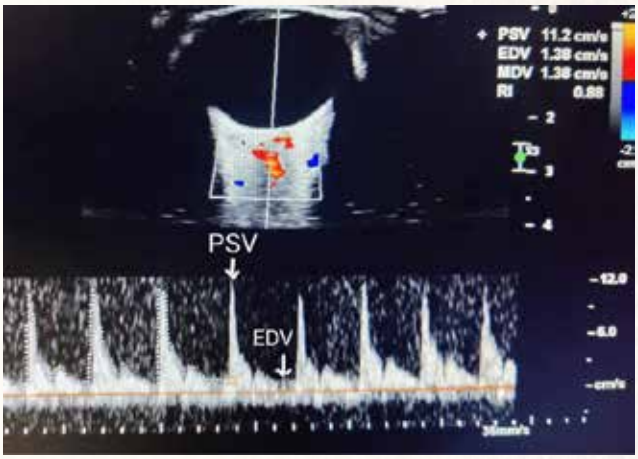

Ophthalmic artery Doppler waveform.

PSV: peak systolic velocity, EDV: end diastolic velocity, MDV: mean diastolic volume, RI: resistive index

Data analysis

Data were entered into a spreadsheet (Excel; Microsoft Inc., Redmond, WA, USA) after coding and processed further using IBM SPSS Statistics for Windows, Version 20.0. (IBM Corp., Armonk, NY, USA). Results are presented using tables. The independent sample Student's t-test was applied to the ophthalmic arteries and Doppler parameters to analyze data among normotensive and preeclamptic pregnant women. A level of statistical significance was established, considering a p-value of less than 0.05 to be statistically significant.

Results

We selected a sample of 80 patients for this study, comprising 50% normotensive individuals (40 patients), 35% with mild preeclampsia (28 patients), and 15% with severe preeclampsia (12 patients). Normotensive participants had a mean

age of 20.8±2.9 years, ranging from 18 to 28 years, whereas the mean age of preeclamptic participants was 27.7±6.3 years, ranging from 18 to 38 years (Table (Table1).1). This difference indicates a higher age of preeclampsia onset in pregnant women.

Table 1

Age distribution of normotensive and hypertensive pregnant women

Maternal age (years)	Normotensive (n)	Hypertensive (n)
<20	24	6
21-30	16	18
31-40	0	16

Gestational age ranged from under 20 weeks to term in normotensive women and from 20 weeks in preeclamptic women (Table (Table2).2). Most women with preeclampsia were in their third trimester, suggesting that mild to severe preeclampsia generally occurs later in pregnancy.

Table 2

Distribution of patients by MAP

MAP: mean arterial pressure

Group	MAP	<20 Weeks	20-28 Weeks	29 Weeks - Term	Total (n)
Normotensive	≤104 mmHg	8	18	14	40
Mild Preeclampsia	105–125 mmHg	0	4	24	28
Severe Preeclampsia	≥126 mmHg	0	2	10	12

We found statistically significant differences in the PI of the normotensive and preeclamptic participants, with mean values of 2.20 to 2.00 and 1.40, respectively ($p<0.05$). Similarly, the EDV in both ophthalmic arteries was statistically significant, with mean EDV values of 8.65 to 8.90 and 16.5 to 16.75 in normotensive and preeclamptic participants, respectively ($p<0.05$). Other Doppler parameters, such as RI, PSV, and mean velocity, showed p-values >0.05, indicating statistical insignificance (Table (Table3).3). The mean OAPI was highest in normotensive pregnant women (2.24) and lowest in the severe preeclamptic group (1.07). This inverse correlation between OAPI and mean maternal arterial pressure suggests reduced orbital vascular resistance and increased orbital flow.

Table 3

Ophthalmic artery velocity parameters in normotensive and preeclamptic pregnant patients.

BP: blood pressure, L.PI: left ophthalmic artery pulsatility index, R.PI: right ophthalmic artery pulsatility index, LPSV: left peak systolic velocity, RPSV: right peak systolic velocity, LMNV: left mean velocity, RMNV: right mean velocity, LDV: left diastolic velocity, RDV: right diastolic velocity, SD: standard deviation, SE: standard error, CI: confidence interval

* 1 = Preeclamptic, 2 = Normotensive

** P<0.05 is considered significant

Parameters	BP *	Mean	SD	SE Mean	95% CI of the Difference		P-Value **
					Lower	Upper	
L.PSV (cm/s)	1	51.00	18.581	4.155	-16.898	2.598	.146
	2	58.15	10.883	2.434	-16.975	2.675	
L.EDV (cm/s)	1	16.55	5.365	1.200	4.952	10.348	.000
	2	8.90	2.594	0.580	4.918	10.382	
L.MNV (cm/s)	1	25.90	9.159	2.048	-0.683	8.683	.092
	2	21.90	4.811	1.076	-0.733	8.733	
L.PI	1	1.40	0.503	0.112	-1.094	-.506	.000
	2	2.20	0.410	0.092	-1.094	-.506	

L.RI	1	0.95	0.375	0.109	-0.368	0.268	.342
	2	1.00	0.000	0.000	-0.650	0.550	
R.PSV (cm/s)	1	54.00	15.865	3.547	-10.630	7.430	.722
	2	55.60	12.093	2.704	-10.651	7.451	
R.EDV (cm/s)	1	16.75	6.958	1.556	4.596	11.604	.000
	2	8.65	3.392	0.758	4.552	11.648	
R.MNV (cm/s)	1	26.00	9.414	2.105	-1.490	8.990	.156
	2	22.25	6.735	1.506	-1.508	9.008	
R.PI	1	1.40	0.503	0.112	-0.828	-0.372	.000
	2	2.00	0.000	0.000	-0.835	-0.365	
R.RI	1	1.05	0.224	0.050	-0.054	0.154	.336
	2	1.00	0.000	0.000	-0.055	0.155	

Discussion

Our findings show that the mean OAPI decreases as pregnancy progresses in both normotensive and preeclamptic individuals. Hence, the OAPI is negatively correlated with gestational age. This decrease in the PI is more pronounced in severely preeclamptic women than in mildly preeclamptic and normotensive women (Table (Table44).

Table 4

Relationship between OAPI and maternal BP.

OAPI: ophthalmic artery pulsatility index, BP: blood pressure, L.PI: left ophthalmic artery pulsatility index, R.PI: right ophthalmic artery pulsatility index

OAPI	Normotensive (n=40)			Mild Preeclampsia (n=28)			Severe Preeclampsia (n=12)		
	Min	Max.	Mean	Min.	Max	Mean	Min	Max.	Mean
L.PI	1.63	2.65	2.20	1.20	2.17	1.61	0.74	1.15	0.98
R.PI	1.73	2.5	2.00	1.23	2.6	1.62	1.00	1.27	1.17

We used ultrasonography to evaluate the maternal ophthalmic artery in normotensive and preeclamptic individuals. We performed color and spectral Doppler studies, collected data from both eyes and analyzed the results. We found statistically significant differences between normotensive and preeclamptic individuals in some Doppler parameters. The PI was lowest in severe preeclampsia (1.17±0.08, $p<0.05$) and highest in normotensive pregnant women (2.92±0.59, $p<0.05$

We also found statistically significant differences in the left and right EDVs. The mean EDV was 16.65 cm/sec in preeclamptic women and 8.77 cm/sec in normotensive women ($p<0.05$). Previous research, such as that by Diniz et al., also found statistically significant differences in EDV ($p=.001$) between mild and severe preeclamptic women and healthy pregnant women [15].

Our study had a few limitations, including a small sample size, based on a survey by Hata et al. [12]. A larger sample size may have produced more precise results [21]. Additionally, the normotensive and preeclamptic women were not matched based on maternal age, gestational age, or other factors that could affect the result. Matching patients could have reduced potential unknown biases. We performed a cross-sectional study; however, a longitudinal study tracking ophthalmic artery changes from early gestation to term might have provided more temporality. Nevertheless, we opted for a cross-sectional design to avoid dropout rates that often accompany longitudinal studies.

Conclusions

Our study found statistically significant differences in the maternal OAPI and EDV in both eyes. We observed that the OAPI inversely correlates with maternal mean arterial blood pressure and gestational age. Both variables indicate decreased vascular resistance and orbital vasodilation, similar to cerebral vessels, since the ophthalmic artery is a branch of the internal carotid artery. Therefore, these parameters can help differentiate between preeclamptic and normotensive pregnancies in late gestation. Given its safety, cost-effectiveness, and accessibility, ultrasonography can be a bedside diagnostic tool.

Accuracy of transrectal strain elastography in detection of prostate cancer

Mangal Subhash Mahajan, Anish Choudhary, Dsouza John, Priscilla C. Joshi

Department of Radiology, Bharati Vidyapeeth Deemed University Medical College, Pune, Maharashtra, India

Abstract

Background: Elastography has emerged as a boon in aiding diagnosis of various neoplastic conditions. Strain elastography helps in differentiating hard lesions from the normal tissue on a real-time basis and targeting biopsies of the same described by other authors in various conditions. We assess a series of cases for the detection of prostate cancer using strain elastography of prostate.

Aims: The aim of this study was to assess the accuracy of transrectal strain elastography in diagnosis of prostate cancer.

Materials and Methods: This is an observational cross-sectional, prospective study. Transrectal strain elastography was performed using a C-10 3 v endocavity probe with elastography software and was compared against biopsy results on 25 adult male patients with raised prostate-specific antigen levels. Statistical significance of qualitative data across two study groups was tested using the Chi-square test or Fisher's exact test. The entire data were analyzed using SPSS version 16.0, Inc., Chicago, software for Microsoft Windows.

Results: Ten (40%) out of 25 patients demonstrated carcinoma prostate, 14 patients had benign prostatic hyperplasia, and 1 had prostatic abscess. Transrectal real-time elastography scores in patients with carcinoma patient were higher than those of benign conditions, i.e., 3 and 4 scores with accuracy of 92%, sensitivity of 85.7%, and specificity of 94.4%.

Conclusions: The overall accuracy of strain elastography was 92%, which enhanced the diagnostic yield in prostate carcinoma. Real-time strain elastography is a highly sensitive and specific technique for diagnosing prostatic carcinoma and guiding the prostate biopsy.

Keywords: Accuracy of elastography, prostate cancer detection, transrectal strain elastography, transrectal ultrasonography prostate

Address for correspondence: Dr. Mangal Subhash Mahajan, Department of Radiology, Bharati Vidyapeeth Deemed University Medical College, Pune-Satara Road, Dhankawadi, Pune - 411 043, Maharashtra, India.
E-mail: drmangalmahajan@gmail.com

INTRODUCTION

Prostate-specific antigen (PSA) levels are raised in prostatic cancer, prostatitis, and benign hyperplasia of the prostate. They are found in levels <4 ng/ml normally in the serum.[1] Carcinoma of prostate (PCa) may be suspected from abnormal PSA levels or digital rectal examination (DRE).[1] Further tests are then performed to reach a diagnosis. Transrectal ultrasonography (TRUS) is often initially performed to detect abnormalities of the prostate and surrounding tissues and to guide biopsy procedures.[2] The

Access this article online	
Quick Response Code:	Website: www.wajradiology.org
	DOI: 10.4103/wajr.wajr_13_18

How to cite this article: Mahajan MS, Choudhary A, John D, Joshi PC. Accuracy of transrectal strain elastography in detection of prostate cancer. West Afr J Radiol 2019;26:31-6.

gold standard being ultrasonography (USG)-guided biopsy followed by histology.[3] Elastography has emerged as a forerunner to assess tissue differences in stiffness. Strain elastography estimates the tissue strain and can distinguish a hard focal lesion from a soft lesion providing an effective alternative to what has been historically qualitatively assessed by palpation.[4] Conventional B mode USG of prostate has a limited role in PCa detection. Even color or power Doppler has a low sensitivity and specificity (40%–50%) for its detection.[5-7] Prostate elastography provides high sensitivity and specificity for detecting PCa with high negative predictive values, thereby ensuring that few cancers will be missed.[8] In this study, we have assessed the accuracy of strain elastography of prostate by performing transrectal real-time strain elastography (TRTE) and comparing it with histopathological findings to reach to a better diagnostic yield.

MATERIALS AND METHODS

The study was approved by the Ethical Committee of the university. A written valid informed consent was obtained for every patient before performing the study. This was a prospective and cross-sectional study conducted on male patients of the age group between 50 and 84 years. The study was carried out over 2 years from August 2015 to 2017. The study group included 25 adult male patients referred to the Department of Radiodiagnosis and Imaging, of a tertiary care university hospital. They had raised serum PSA levels and clinically suspected to have PCa. All these patients underwent TRTE followed by prostate biopsy. Diagnoses were confirmed by histopathological examination of the specimen.

Elastography imaging

TRTE was performed using Philips iU22 ultrasound system with elastography software, and C10 3 v endocavity broadband curved array (C10-3 v) probe was used for B-mode biopsy and TRTE examinations.

The subjects were studied using the following protocol:

- Four hours fasting before the study
- The patient was placed in the left lateral position with bent knees and hip flexion
- Adequate amount of 2% lignocaine jelly was introduced in the anal canal and applied to the anal vergeto get good local anesthetic effect before inserting the C10 3 v probe
- The C10 3 v probe was covered with latex covering with adequate coupling agent in between and the probe was inserted in the rectum after initial milking to relax the anal sphincter
- The morphology of prostate gland, symmetry, and the capsule was initially assessed by grayscale ultrasound. Any focal lesion, asymmetry, capsular bulge, and diffuse alteration in gland echotexture were recorded. Color Doppler and power Doppler ultrasound modes were then used to detect any blood flow abnormality in the gland
- Strain elastography was then carried out. Each section was checked from the apex to base on both sides. The images were obtained in the transverse plane at up to 10 frames per second with focus at a depth of 1.5 cm from the surface of the probe. The region of interest of elastography was set at approximately 1 cm to the edge of the largest transverse image
- Manual compression and decompression of the prostatic tissue were carried out using the C10 3 v probe. Under the guidance of quality bar in the process of compression and decompression, the pressure and direction of manual vibration were adjusted until stable, repeatable images were obtained. The images were recorded for further interpretation and comparison
- Examination time for each patient was about 10–15 min.

Image interpretation and score assignment

Normal prostatic and soft tissues appeared red to green [Figure 1] on elastogram. The hard prostatic tissue appeared blue [Figures 2 and 3].

Elastographic score was assigned to each of the patient's elastogram. Elastography score – 1, 2, 3, 4, or 5 was assigned in accordance with values provided by Xu *et al*.:[8]

- A. Score 1: There was no blue area or star-like blue in outer glands

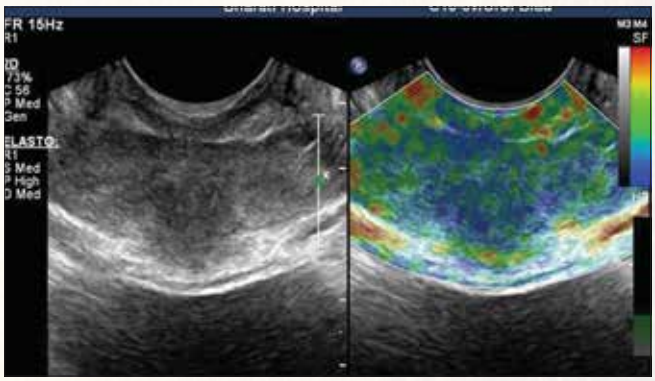

Figure 1: Transverse B-mode and elastography images in a 29-year-old control male with normal serum prostate-specific antigen level. B-mode ultrasound (right) shows normal prostate gland. Corresponding elastogram (left) shows no focal hardening of the peripheral zones of the prostate. Transrectal real-time strain elastography score 1 - there was no blue area or star-like blue in outer glands

- B. Score 2: The mosaic or a little symmetrical blue area in bilateral outer glands were seen, and the blue area is <5 mm in diameter
- C. Score 3: A little symmetrical blue area in bilateral outer glands, the diameter of blue area ≥5 mm
- D. Score 4: Asymmetric blue area in bilateral outer glands, the diameter of blue area ≥5 mm
- E. Score 5: Asymmetric blue area in bilateral outer glands, the blue area of more than 50%, and the blue area ≥50% of single outer gland area.

Prostatic biopsy

All patients underwent TRUS-guided 12 core prostate biopsy using 18G true cut biopsy gun under all aseptic precautions. All focal hard lesions suspected on elastogram were also targeted.

Statistical analysis

Data on qualitative characteristics are presented as *n* (% of cases). The statistical significance of difference of qualitative characteristics across two study groups was tested using the Chi-square test or Fisher's exact test. The diagnostic efficacy indices, such as sensitivity, specificity, positive predictive value (PPV), negative predictive value (NPV), and accuracy, were calculated for the test method against the gold standard of histopathology. Accuracy measure along with 95% confidence interval (CI) is also presented for each agreement analysis. To determine the extent and significance of agreement between the test methods and the gold standard, Cohen's Kappa Statistic was used.

$P < 0.05$ is considered to be statistically significant. All the hypotheses were formulated using two-tailed alternatives against each null hypothesis (hypothesis of no difference). The entire data were statistically analyzed using Statistical Package for Social Sciences (SPSS version 16.0, Inc., Chicago, IL, USA) for Microsoft Windows.

RESULTS

The most common age group involved, in this study, was between 61 and 70 years followed by the age group of 71–80 years [Table 1]. The mean ± standard deviation, median (minimum–maximum) age of the entire study group is 66.1 ± 7.55 and 65.0 (50.0–84.0) years, respectively.

Table 1: Age distribution in patients with raised prostate-specific antigen values (*n*=25)

Age group (years)	Number of patients (%)
41-50	1 (4.0)
51-60	4 (16.0)
61-70	13 (52.0)
71-80	6 (24.0)
81-90	1 (4.0)
Total	25 (100.0)

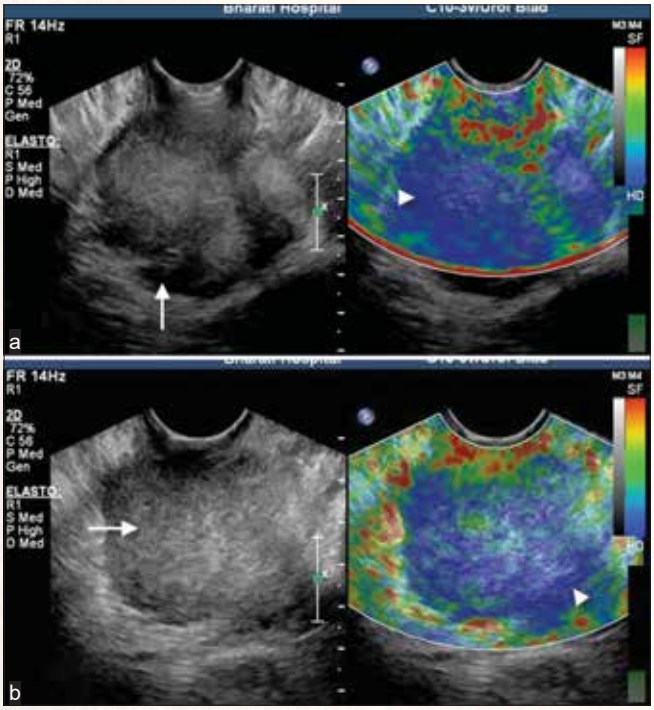

Figure 2: (a and b) Transverse B-mode and elastography images in a 75-year-old male. Digital rectal examination revealed Grade III hard prostate. Serum prostate-specific antigen was 148 ng/ml. B-mode image (right) shows prostatomegaly, heterogeneous echogenicity, and loss of normal zonal anatomy of prostate (arrow in a and b). Transrectal real-time strain elastography image (left) shows asymmetric blue area in bilateral outer glands, the diameter of blue area ≥5 mm (arrowhead in a and b). Biopsy revealed adenocarcinoma with Gleason Score (4 + 3) = 7

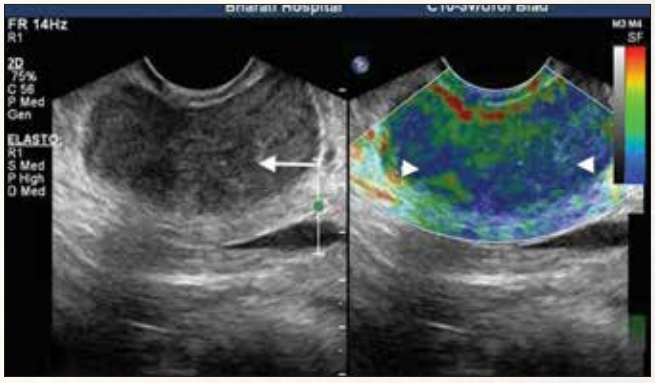

Figure 3: Transverse B-mode and elastography images in a 69-year-old male. Urgency and frequency of micturition with raised serum prostate-specific antigen prostate-specific antigen of 16 ng/ml. B-mode image (right) shows mild heterogeneous echotexture of the prostate (arrow). No focal hardening of the peripheral zones of the prostate on elastography (left). The mosaic or a little symmetrical blue area in bilateral outer glands, the blue area is <5 mm in diameter (arrowhead). Biopsy revealed benign hyperplasia of prostate with acute prostatitis

The most common serum PSA range, in our study, was between 11 and 50 ng/mL followed by values more than 100 ng/ml [Table 2].

In total, 10 of 25 patients (40%) were diagnosed with prostate cancer [Graph 1]. The Gleason score ranged from 4 to 7.

The TRTE scores of PCa and benign conditions were 3.20 ± 1.11 (range: 1–5) and 2.24 ± 1.01 (range: 1–4), respectively [Table 3]. The mean TRTE score of PCa was significantly higher than that of benign conditions ($P < 0.001$).

For screening of PCa, the sensitivity, specificity, PPV, and NPV of elastography compared to histopathology examination were 85.7%, 94.4%, 85.7%, and 94.4%, respectively. The overall accuracy (with 95% CI) of elastography against histopathology examination was 92.0% (81.4%–99.9%) [Graph 2 and Table 4].

Table 2: Distribution of serum prostate-specific antigen values in patients with suspected prostate cancer (*n*=25)

Serum PSA (ng/mL)	Number of patients (%)
4-10	2 (8.0)
11-50	19 (76.0)
51-100	1 (4.0)
>100	3 (12.0)
Total	25 (100.0)

PSA - Prostate-specific antigen

Table 3: Cross tabulation of elastography transrectal real-time strain elastography findings with biopsy (Gleason's score)

Gleason score (biopsy) versus TRTE cross-tabulation					
	Elastography score				Total
Biopsy score Gleason	1	2	3	4	
4	1	0	0	0	1
5	0	2	0	0	2
6	0	0	0	0	0
7	0	0	4	3	7
>7	0	0	0	0	0
Total	1	2	4	3	10

TRTE - Transrectal real-time strain elastography

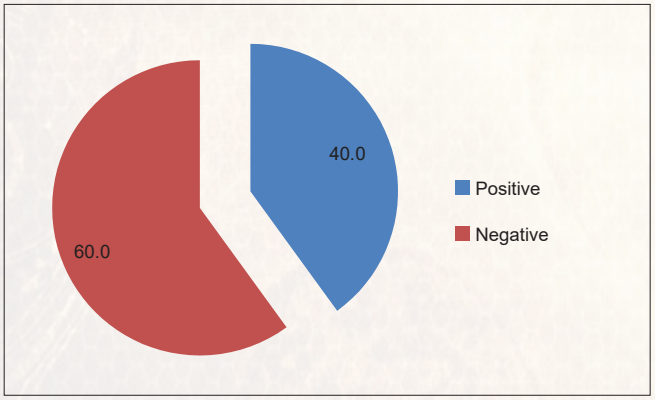

Graph 1: Distribution of patients (%) positive for carcinoma of prostate (biopsy proven)

DISCUSSION

Prostate cancer is one of the most common cancers in men in Western countries and stands the second position in male malignant tumors worldwide.[9] The incidence and prevalence of PCa have increased significantly since the last decade.[10,11] The diagnostic evaluation of PCa comprises of serum PSA level, DRE, and diagnostic imaging methods such as ultrasound and magnetic resonance imaging. Approximately 85% of PCa is multifocal and progresses along the prostate capsule, and it may not appear as a well-defined nodule such as other malignant tumors.[12] The ideal imaging technology should be both affordable and minimally invasive. Prostate biopsy is invasive, costly, and involves risk of complications. Therefore, the focus is required to improve prostate imaging that can be noninvasive and cost-effective. It can be achieved using real-time strain elastography. Elastography being noninvasive, easily available, cost-effective, and less time-consuming can be used as a screening tool in evaluation of PCa.[13-15]

In the nineties, Ophir *et al*. used elastography for biological tissues since then it has undergone many modifications,[16] and now TRTE is chiefly used to differentiate malignant hard lesions from soft lesions[15] and guiding transrectal prostate biopsies[8,17-19] as a new technique for better diagnostic yield in PCa. Patients with raised serum PSA levels, abnormal DRE with focal abnormal nodules on conventional ultrasound can be diagnosed by TRUS-guided biopsy targeting the nodule. However, for the patients with only elevated PSA levels without focal abnormalities, it remains unclear whether all quadrant biopsies are necessary. In such a group of patients by identifying hard tissue on elastogram, TRTE can increase the accuracy of biopsy, reduce the

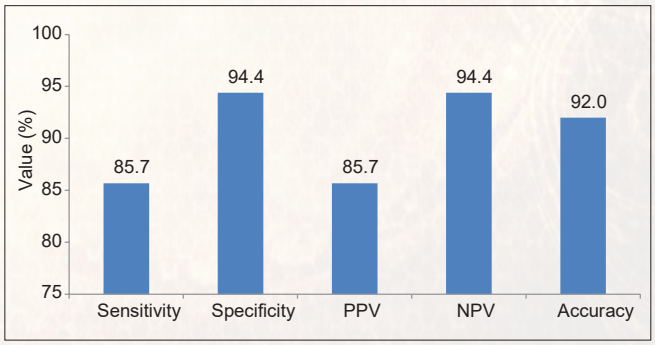

Graph 2: The distribution of indices of diagnostic efficacy of elastography against histopathology examination as a Gold Standard (*n* = 25)

Table 4: The sensitivity and specificity analysis for the diagnosis of prostatic carcinoma based on elastography against the histopathology (Gleason score - gold standard) (*n*=25)

Elastography	Histopathology		Total, *n* (%)	Diagnostic efficacy indices (%)				
	Positive, *n* (%)	Negative, *n* (%)		Sensitivity	Specificity	PPV	NPV	Accuracy (95% CI)
Positive	6 (85.7)	1 (5.6)	7 (28.0)	85.7	94.4	85.7	94.4	92.0 (81.4-99.9)
Negative	1 (14.3)	17 (94.4)	18 (72.0)					
Total	7 (100)	18 (100)	25 (100)					

Values are *n* (% of cases). Cohen's Kappa value=0.802, *P*=0.001*** (statistically highly significant). PPV - Positive predictive value; NPV - Negative predictive value; CI – Confidence interval

number of biopsy cores, and eventually reducing the complication rate and pain to the patient. Cell density is greater in neoplastic tissue as compared to normal tissue which causes a change in tissue elasticity.[20] TRTE allows an assessment of tissue elasticity with color coding, in which, the scale ranged from red (soft) to blue (hard). Kamoi *et al*.,[21] initially, reported that the grading system of TRTE was valuable in the diagnosis of PCa, and this was successfully applied to breast lesions and thyroid nodules.[21,22] In the clinical application of TRTE-guided biopsy, hard areas with a diameter ≥5 mm in elasticity imaging were considered as malignant.[23,24] Many prostate cancers detected at biopsy were not visible at TRUS as many cases had isoechoic lesions.[21] Therefore, the TRTE score based on the symmetry, and elastic distribution of prostate helped in both diagnosis and focused biopsy guidance.

In this study, the mean TRTE score of PCa was significantly higher than that of benign conditions. The sensitivity, specificity, and overall accuracy of TRTE (with 95% CI) in diagnosis of PCa were 85.7%, 94.4%, and 92%, respectively. On the other hand, in the study of Kamoi *et al*.,[21] the sensitivity, specificity, and accuracy of the grading system of TRTE focused on prostate lesions were 68%, 81%, and 76%, respectively. The difference between the studies could be attributable to the large sample of the latter, namely *n* = 107 cases as compared to *n* = 25 in this study. Therefore, it may be valuable to introduce TRTE into routine clinical practice for the detection of the lesion and as a guide to biopsy. In the present study, TRTE detection rate of prostate cancer with a higher Gleason score was higher than that of lower Gleason score which compared favorably to studies of Kamoi *et al*.,[21] Aigner *et al*.,[18] and Spârchez.[11]

CONCLUSIONS

Our study has provided a higher level of confidence to use real-time strain elastography as an imaging tool to evaluate patients with raised serum PSA levels to enhance the diagnostic yield for the detection of prostate cancer. It can also be a good adjuvant to guide TRUS biopsy to avoid error.

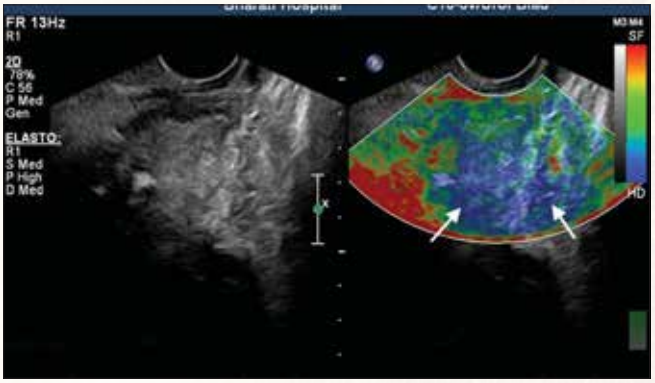

Figure 4: Transrectal real-time strain elastography can produce hard artifacts (arrow) with increasing depth of penetration

Limitations and pitfalls

The major limitation of TRTE is that the procedure of manually compressing the prostate gland is operator-dependent as brought out by the study of Miyagawa *et al*.[25]

Pelzer *et al*.[26] and Pallwein *et al*.[24] reported that TRTE could produce hard artifacts [Figure 4] with increasing depth of penetration.

The third limitation was that biopsy specimen cannot diagnose all the PCa due to the sampling error.

Declaration of patient consent

The authors certify that they have obtained all appropriate patient consent forms. In the form the patient(s) has/have given his/her/their consent for his/her/their images and other clinical information to be reported in the journal. The patients understand that their names and initials will not be published and due efforts will be made to conceal their identity, but anonymity cannot be guaranteed.

Financial support and sponsorship

Nil.

Conflicts of interest

There are no conflicts of interest.

REFERENCES

1. Catalona WJ, Richie JP, Ahmann FR, Hudson MA, Scardino PT, Flanigan RC, *et al.* Comparison of digital rectal examination and serum prostate specific antigen in the early detection of prostate cancer: Results of a multicenter clinical trial of 6,630 men. J Urol 1994;151:1283-90.
2. Romics I. Ultrasound guided biopsy, a gold standard diagnostical test of the prostate cancer. Acta Chir Iugosl 2005;52:23-6.
3. Flanigan RC, Catalona WJ, Richie JP, Ahmann FR, Hudson MA, Scardino PT, *et al.* Accuracy of digital rectal examination and transrectal ultrasonography in localizing prostate cancer. J Urol 1994;152:1506-9.
4. Bamber J, Cosgrove D, Dietrich CF, Fromageau J, Bojunga J, Calliada F, *et al.* EFSUMB guidelines and recommendations on the clinical use of ultrasound elastography. Part 1: Basic principles and technology. Ultraschall Med 2013;34:169-84.
5. Rifkin MD, Zerhouni EA, Gatsonis CA, Quint LE, Paushter DM, Epstein JI, *et al.* Comparison of magnetic resonance imaging and ultrasonography in staging early prostate cancer. Results of a multi-institutional cooperative trial. N Engl J Med 1990;323:621-6.
6. Beerlage HP, Aarnink RG, Ruijter ET, Witjes JA, Wijkstra H, Van De Kaa CA, *et al.* Correlation of transrectal ultrasound, computer analysis of transrectal ultrasound and histopathology of radical prostatectomy specimen. Prostate Cancer Prostatic Dis 2001;4:56-62.
7. Langer DL, van der Kwast TH, Evans AJ, Trachtenberg J, Wilson BC, Haider MA, *et al.* Prostate cancer detection with multi-parametric MRI: Logistic regression analysis of quantitative T2, diffusion-weighted imaging, and dynamic contrast-enhanced MRI. J Magn Reson Imaging 2009;30:327-34.
8. Xu G, Feng L, Yao M, Wu J, Guo L, Yao X, *et al.* A new 5-grading score in the diagnosis of prostate cancer with real-time elastography. Int J Clin Exp Pathol 2014;7:4128-35.
9. Jemal A, Bray F, Center MM, Ferlay J, Ward E, Forman D, *et al.* Global cancer statistics. CA Cancer J Clin 2011;61:69-90.
10. Hsing AW, Tsao L, Devesa SS. International trends and patterns of prostate cancer incidence and mortality. Int J Cancer 2000;85:60-7.
11. Spârchez Z. Real-time ultrasound prostate elastography. An increasing role in prostate cancer detection? Med Ultrason 2011;13:3-4.
12. McNeal JE, Redwine EA, Freiha FS, Stamey TA. Zonal distribution of prostatic adenocarcinoma. Correlation with histologic pattern and direction of spread. Am J Surg Pathol 1988;12:897-906.
13. Cochlin DL, Ganatra RH, Griffiths DF. Elastography in the detection of prostatic cancer. Clin Radiol 2002;57:1014-20.
14. Lyshchik A, Higashi T, Asato R, Tanaka S, Ito J, Mai JJ, *et al.* Thyroid gland tumor diagnosis at US elastography. Radiology 2005;237:202-11.
15. Garra BS, Cespedes EI, Ophir J, Spratt SR, Zuurbier RA, Magnant CM, *et al.* Elastography of breast lesions: Initial clinical results. Radiology 1997;202:79-86.
16. Ophir J, Céspedes I, Ponnekanti H, Yazdi Y, Li X. Elastography: A quantitative method for imaging the elasticity of biological tissues. Ultrason Imaging 1991;13:111-34.
17. Kapoor A, Kapoor A, Mahajan G, Sidhu BS. Real-time elastography in the detection of prostate cancer in patients with raised PSA level. Ultrasound Med Biol 2011;37:1374-81.
18. Aigner F, Pallwein L, Junker D, Schäfer G, Mikuz G, Pedross F, *et al.* Value of real-time elastography targeted biopsy for prostate cancer detection in men with prostate specific antigen 1.25 ng/ml or greater and 4.00 ng/ml or less. J Urol 2010;184:913-7.
19. Ferrari FS, Scorzelli A, Megliola A, Drudi FM, Trovarelli S, Ponchietti R, *et al.* Real-time elastography in the diagnosis of prostate tumor. J Ultrasound 2009;12:22-31.
20. Krouskop TA, Wheeler TM, Kallel F, Garra BS, Hall T. Elastic moduli of breast and prostate tissues under compression. Ultrason Imaging 1998;20:260-74.
21. Kamoi K, Okihara K, Ochiai A, Ukimura O, Mizutani Y, Kawauchi A, *et al.* The utility of transrectal real-time elastography in the diagnosis of prostate cancer. Ultrasound Med Biol 2008;34:1025-32.
22. Itoh A, Ueno E, Tohno E, Kamma H, Takahashi H, Shiina T, *et al.* Breast disease: Clinical application of US elastography for diagnosis. Radiology 2006;239:341-50.
23. König K, Scheipers U, Pesavento A, Lorenz A, Ermert H, Senge T, *et al.* Initial experiences with real-time elastography guided biopsies of the prostate. J Urol 2005;174:115-7.
24. Pallwein L, Mitterberger M, Struve P, Pinggera G, Horninger W, Bartsch G, *et al.* Real-time elastography for detecting prostate cancer: Preliminary experience. BJU Int 2007;100:42-6.
25. Miyagawa T, Tsutsumi M, Matsumura T, Kawazoe N, Ishikawa S, Shimokama T, *et al.* Real-time elastography for the diagnosis of prostate cancer: Evaluation of elastographic moving images. Jpn J Clin Oncol 2009;39:394-8.
26. Pelzer AE, Bektic J, Berger AP, Halpern EJ, Koppelstätter F, Klauser A, *et al.* Are transition zone biopsies still necessary to improve prostate cancer detection? Results from the Tyrol screening project. Eur Urol 2005;48:916-21.

SCIENTIFIC WRITE UP

CARDIAC MRI : WHAT THE RADIOLOGIST SHOULD TAKE CARE

Dr. Vineeta Ojha (Consultant Mahajan Imaging, Ex-Asst. Prof. AIIMS DELHI)

Cardiac MRI represents a pivotal tool in the armamentarium of diagnostic imaging, offering unparalleled insights into the heart's structure, function, and tissue characteristics without the use of ionizing radiation. For radiologists, it's essential to grasp the fundamentals of this technique, including the principles of magnetic resonance imaging specific to the cardiac domain, patient safety considerations, and the nuances of various imaging protocols tailored to answer clinical questions. Mastery of cardiac MRI involves understanding how to leverage its high spatial and temporal resolution to evaluate myocardial viability, ventricular function, and complex congenital heart diseases. Furthermore, knowledge of the limitations, such as the need for patient cooperation and potential contraindications in patients with certain implants, is vital. As cardiac MRI continues to evolve, staying abreast of technological advancements and their clinical applications will enable radiologists to provide comprehensive care, guiding patient management through accurate diagnosis and assessment of therapeutic efficacy.

Common indications for a cardiac MRI range from diagnosing various cardiomyopathies, assessing ischemic heart disease and myocardial viability, to evaluating complex congenital and valvular heart diseases. CMR is also crucial for characterizing cardiac masses, identifying the extent of myocardial inflammation in conditions like myocarditis, and delineating vascular diseases such as aortic aneurysms and dissection. Furthermore, it provides invaluable insights into pericardial diseases, aids in the detection of arrhythmogenic substrates, and evaluates heart failure and cardiac remodelling. The technique employs a variety of sequences to achieve its diagnostic goals: Cine MRI for assessing ventricular function and wall motion; Late Gadolinium Enhancement (LGE) for detecting myocardial fibrosis or scarring indicative of ischemic injury or cardiomyopathy; T1 and T2 mapping for detailed tissue characterization, allowing for the differentiation of various types of myocardial involvement; and Phase-contrast MRI for evaluating blood flow and valvular function. In the context of cardiomyopathies, cardiac MRI holds significant prognostic utility; the presence and extent of LGE can predict adverse outcomes, including arrhythmias, heart failure progression, and sudden cardiac death. This modality's ability to precisely quantify ventricular volumes, ejection fraction, and myocardial fibrosis offers invaluable insights into disease severity, progression, and response to therapy, enabling personalized patient management and prognostication.

Breast Imaging From Basics to Advanced

Dr Prof Shabnam Bhandari Grover
SMSR, Sharda Hospital, Sharda University, Greater Noida, Delhi-NCR.

Around the world breast cancer is the leading cause of cancer, and contributes to 25% of all female cancers. It has been estimated by experts, that breast cancer deaths in the South-East Asia region are likely to have a phenomenal rise to 61.7% by 2040. In India breast cancer is the most common cancer of all female cancers, accounting for 28.2% of all the female cancers. The incidence rate of female breast cancer has increased in India, by 39.1% from 1990 to 2016, in all geographic regions of India. Further, it is documented by statistical surveys and studies that breast cancer deaths in India, occur with a higher proportion of 70 %, in patients younger than 70 years and India has a much lower 5 year survival rate for breast cancer, compared to Western countries. Over 70% of the afflicted women present in advanced stage of disease, which is the major factor behind the high rate of mortality in India. The importance of a robust knowledge of breast imaging for both, screening and diagnosis, therefore needs no further emphasis.

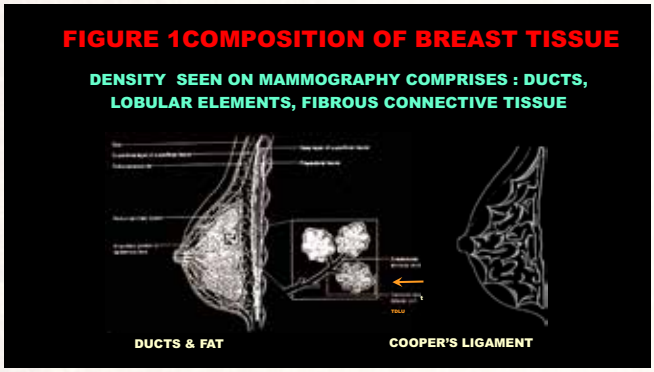

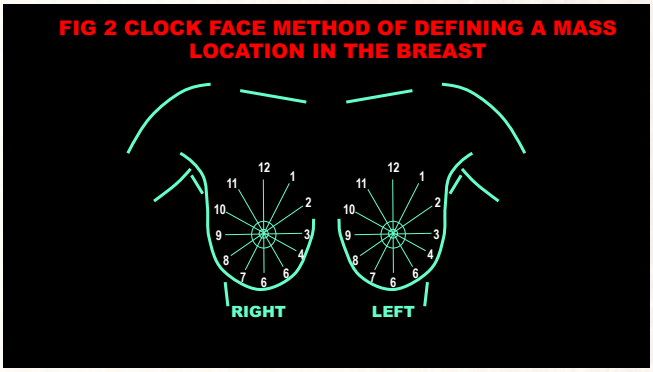

The western countries all have a breast cancer screening program, which facilitates early detection of cancer at a non-palpable stage and thus contributes to better treatment outcomes and improved disease-free survival. Unfortunately, India lacks a screening program and the best all specialty physicians can contribute is to proactively counsel all colleagues, family members and family friends to overcome hesitation and go forward with annual mammography from the age of 40 years till 70 years. A white paper from National Academy of Medical Sciences, recommends annual mammography for all asymptomatic women, from the age of 40 years till 70 years. For pregnant and lactating women and women below thirty years of age, breast ultrasound is the investigation of choice. For women between thirty to thirty-nine years of age, it is recommended to perform ultrasound initially followed by mammography, both in asymptomatic women or if there is a clinical or a sonographic suspicion of breast cancer.

The lecture this lecture aims to clarify, which patient needs only mammography (MG), which patient needs both mammography & Ultrasound, which patient needs only ultrasound & color doppler and we also highlight the specific role ultrasound elastography and Contrast Enhanced Ultrasound (CEUS) in breast diseases. We also introduce the important role of CT/ PET CT in breast diseases as well as the role MRI / PET MRI in breast diseases.

As already highlighted above, mammography is the recommended modality for diagnosis in any symptomatic patient above 40 years and for Screening for malignancies in patients above 40 years. Ultrasound further evaluation in a mass diagnosed in a symptomatic patient or on a screening mammogram. Ultrasound has an important role for further evaluation of the diagnosed mass as solid or cystic, other gray scale features, color doppler, ultrasound elastography and CEUS features further characterize a mass as benign or malignant.

The mammography equipment requires uniform low energy radiation. Low energy helps to exaggerate contrast between the soft tissues comprising breast structures. This achieved by using a Molybdenum anode, which produces 17.9-19.5 kev radiation and a Molybdenum filter absorbs any energy > 20 kev. Thus, filtration results

in a uniform spectrum of energy. The density seen on mammography comprises: ducts, lobular elements, fibrous connective tissue as shown in Figure 1. The abnormalities detected on Mammography or ultrasound are described by the clock face method as shown in figure 2. The breast parenchyma and composition are described as per the latest BIRADS Edition of 2013, known as BIRADS fifth edition, as summarized in table 1. The BIRADS classification of breast abnormalities is shown in Table 2. Majority of the BIRADS parameters, will be illustrated with images of real-life cases examined by the Author.

Digital breast tomosynthesis (DBT) is an advancement of mammography, which involves multiple projections of mammographic information, acquired across an arc that are reconstructed into a series of stacked images. Depending on the manufacturer, during DBT image acquisition, the x- ray tube pivots in an arc that varies between 15° (narrow range) and 60° (wide range) in a plane aligned to the chest wall. In general, the larger angular range of the x-ray tube motion results in more tomographic information and yields better section separation or vertical resolution. DBT allows differentiation between false and true masses, exact morphology of the suspected mass, true architectural distortion, types of calcification and the true number of masses, which may not be detected on 2D examination, if they are overlapping masses.

Gray scale sonograph criteria for d/d between benign and malignant breast lesion was defined by Stavros et al, in 1995. Masses with Irregular/angulated margins, spiculation micro-lobulations, even on single surface, a mass being taller than wider (anti parallel), a mass with duct extension, Hypoechoic nature, internal echotexture being heterogenous, posterior acoustic shadowing, thick edge shadows presence of calcifications, and vascularity on Color Doppler, all favor malignancy. All applications will be illustrated with images of real-life cases examined by the Author.

Ultrasound Elastography is an imaging technique which quantifies hardness of any lesion, in relation to its surrounding tissue. The principle is that compression produces strain within tissue and the Strain is smaller in harder tissue than softer tissue, therefore it is useful in d/d benign vs malignant masses: as malignant lesions have an increased hardness, deform less, and also show larger dimensions on elastography. Benign masses on the other hand, have a low hardness and deform more in comparison to malignant masses, and appear smaller

TABLE 1

AMERICAN COLLEGE OF RADIOLOGY (ACR BIRADS 5TH EDITION, 2013)

BREAST IMAGING REPORTING AND DATA SYSTEMS

ACR a	PREDOMINANTLY FAT, RADIOLUCENT BREAST
ACR b	SCATTERED FIBRO -GLANDULAR DENSITIES
ACR c	SHOWS HETEROGENOUSLY DENSE PATTERN WHICH MAY OBSURE SMALL MASSES
ACR d	EXTREMELY DENSE PARENCHYMA WHICH LOWERS SENSITIVITY OF MAMMOGRAPHY

TABLE 2

ACR CLASSIFICATION OF BREAST ABNORMALITIES

BREAST IMAGING REPORTING AND DATA SYSTEMS (BIRAD 2013)

BIRADS	0	NEEDS FURTHER EVALUATION
BIRADS	1	NORMAL STUDY
BIRADS	2	BENIGN FINDINGS
BIRADS	3	PROBABLY BENIGN
BIRADS	4	SUSPICIOUS FOR MALIGN : A-LOW SUSPICION
		B-MODERATE SUSPICION
		C-HIGH SUSPICION
BIRADS	5	HIGHLY SUGGESTIVE OF MALIGNANCY
BIRADS	6	BIOPSY PROVEN MALIGNANCY

on the elastogram. All applications will be illustrated with images of real-life cases examined by the Author. The reader is advised to refer to our publication, on principles of elastography, listed in references, for a better understanding of the subject.

CEUS is useful for better characterization BIRADS 3 and 4 masses, Pre surgical prediction of prognostic factors and for Pre and post Neo Adjuvant Chemotherapy (NAC) response assessment. All applications will be illustrated with images of real life cases examined by the Author.

The role of MRI in breast cancer, is for evaluation for multifocal (same quad) / multicentric (different quadrant) disease in a diagnosed case. Evaluation of the chest wall invasion in breast cancer is also an important component of comprehensive local staging of breast cancer. Staging of axillar lymph node using contrast enhancement, post resection evaluation of a patient with positive margins after resection, are other important indications of breast

MRI. Additionally, breast MRI is useful for differential diagnosis between, residual and recurrent disease in a treated patient. Finally, MRI is the recommended modality for breast screening in any woman with family history of breast cancer. All applications will be illustrated with images of real life cases examined by the Author.

BIBLIOGRAPHY/ REFERENCES

1. Sathishkumar K, Sankarapillai J, Mathew A, et al. Breast cancer survival in India across 11 geographic areas under the National Cancer Registry Programme. Cancer. 2024; 1-10. doi:10.1002/cncr.35188

2. Singh S, Shrivastava JP, Dwivedi A. Breast cancer screening existence in India: A nonexisting reality. Indian J Med Paediatr Oncol. 2015 Oct-Dec;36(4):207-9. doi: 10.4103/0971-5851.171539. PMID: 26811588; PMCID: PMC4711217.

3. Chakrabarthi S, Panwar S, Singh T, Lad S, Srikala, Khandelwal N, Misra S, Thulkar S. Best Practice Guidelines for Breast Imaging, Breast Imaging Society, India: Part-1. Ann Natl Acad Med Sci (India) 2022;58:60-68.

4. Patra S, Grover SB. Physical Principles of Elastography: A Primer for Radiologists. Indographics 2022;1:27–40. (An IJRI- IRIA publication, Open Access).

Percutaneous transhepatic biliary drainage: Indications and Technique

Dr. Rajeev N Priyadarshi (Prof. AIIMS PATNA)

Percutaneous Transhepatic Biliary Drainage (PTBD) is a radiological interventional procedure performed for biliary drainage by inserting a biliary catheter through a peripheral intrahepatic biliary duct under image guidance. This procedure involves percutaneous insertion of a catheter or stent into the biliary system, typically under ultrasound and fluoroscopic guidance.

Biliary drainage is indicated for patients with biliary obstruction, typically presenting with clinical jaundice and pruritus, which can significantly impact quality of life. It is a lifesaving procedure for cholangitis, often resulting from previous biliary procedures. Postoperative bile leaks and anastomotic strictures following liver or pancreatic surgery may also necessitate biliary drainage for diversion of bile and management of complications.

PTBD can be performed with external drainage, where a catheter is left outside the body to facilitate bile drainage, or internal drainage, where an internal- external catheter or a self-expandable metallic stent is placed across the obstruction to restore biliary flow. Internal-external biliary drainage is preferred over external drainage when possible. The catheter is positioned to allow internalization of the drainage, which offers stability and reduces the risk of dislodgement. Additionally, internal-external drainage is more physiologic, improves quality of life, and reduces the risk of skin complications. If internalization is not possible initially, attempts can be made after a few days of PTBD once biliary dilation and edema have decreased.

Before PTBD, imaging studies are carefully reviewed to determine the type and cause of the obstruction. Planning involves deciding on the approach (right, left, bilateral, or multiple catheter drainage) based on the specific situation and treatment goals. When reducing bilirubin levels is the goal, draining at least 30% of liver volume with a single catheter is typically aimed for.

Technique

The PTBD procedure typically begins percutaneous access of the biliary duct as performed for percutaneous transhepatic cholangiography (PTC). A 22G Chiba needle is usually used to puncture dilated bile ducts under ultrasound guidance. After opacification of the biliary system with contrast, a 0.018-in nitinol guidewire is advanced into the biliary duct, followed by insertion of a coaxial introducer set. Subsequently, a 0.035-in hydrophilic guidewire is inserted into the bile duct and exchanged for a stiff wire, over which a drainage catheter is inserted after tract dilation. Using angled tip catheter and hydrophilic guidewire the obstructed system is negotiated and subsequently catheter is advanced over a hydrophilic wire beyond the obstruction into duodenum. Finally, over a stiff wire a catheter with multiple side holes (Ring-Biliary catheter) is placed into the duodenum. During the procedure, fluoroscopy is used to cross the obstructed segment and to access into duodenum. In emergencies, such as severe cholangitis, external drainage may be performed without fluoroscopy when the bile ducts are significantly dilated.

For inoperable malignant biliary obstructions, internal drainage with self-expandable metallic stents is a common palliative treatment option. Bilateral stenting may be necessary for hilar obstructions to adequately decompress both liver lobes. Careful planning and technique are crucial for successful stent deployment.

PTBD generally has a high success rate, but complications like hemorrhage and cholangitis/sepsis can occur, albeit rarely. Other issues may include biliary leakage or decreased bile output, which are managed accordingly with interventions like catheter repositioning or replacement.

In summary, PTBD is an effective procedure for relieving biliary obstruction, with manageable risks when performed with proper patient selection, meticulous technique, and careful post-procedural care.

Budd–Chiari syndrome: Imaging and Interventional management

Budd–Chiari syndrome (BCS) is an uncommon condition of the liver characterized by the obstruction of the hepatic venous outflow tract, leading to congestion within the liver. This obstruction can occur at any point

between the small hepatic veins and the right atrium of the heart, resulting in what is also known as hepatic venous outflow tract obstruction (HVOTO). BCS can be either primary or secondary. Primary BCS arises from intrinsic venous problems due to inherited or acquired hypercoagulable states, while secondary BCS can occur due to compression or invasion of the venous outflow tract due to abscesses, tumors or other lesions. In our experience the typical symptoms of BCS are always due to primary BCS; secondary cases are neither symptomatic nor their treatment follows the typical management.

The pathophysiology of BCS involves increased sinusoidal pressure due to venous stasis, leading to hepatic sinusoidal thrombosis and subsequent reduction in hepatic perfusion. This reduction in blood flow can result in ischemia and necrosis of hepatocytes, particularly in perivenular zones, leading to fibrosis and the development of portal hypertension.

It is imperative that radiologists be fully versed with the imaging features and its interventional management as the diagnosis of this condition is totally based on imaging findings; biopsy is rarely performed for the diagnosis purpose. The diagnosis of BCS is often delayed as many of the cases we have seen are being misdiagnosed as chronic liver disease due to other causes. Also, in our experience medical treatment fails in most cases and surgery is almost absolute nowadays for the management of this condition. Although liver function tests are often abnormal in severe cases, mild cases may have normal tests. Clinical presentations are often classified as acute (less than 2 months), subacute (less than a year) or chronic (more than a year).

Imaging findings in BCS primarily depend on congestion and the development of venous collaterals. In acute disease, congestion is pronounced, and collateral development is limited. Major vein occlusion leads to congestion and poor perfusion in the peripheral portion of the liver, resulting in patchy enhancement or hypoenhancement. The caudate lobe may enlarge even in acute disease. Thrombus visible in a minority of cases. Patients with acute BCS typically present with massive ascites, tender hepatomegaly, and abnormal liver function tests. In chronic cases, peripheral segments may atrophy, and the caudate lobe or other well perfused segments may hypertrophy. Intrahepatic collaterals, known as bridging or veno-venous collaterals, develop, and focal hepatic lesions such as regenerative nodules may appear hypervascular in arterial phase imaging.

Radiological interventions for BCS include angioplasty of the inferior vena cava (IVC) and/or hepatic vein, HV/IVC stenting, and direct intrahepatic portocaval shunts (DIPS). Angioplasty is performed for short-segment stenosis or membranous obstruction, typically accessed via femoral or jugular venous access. Stent placement is considered for long-segment stenosis or significant residual stenosis post-angioplasty. In cases where recanalizable hepatic veins are unavailable or prior procedures have failed, TIPS/DIPS procedures are necessary to provide venous outflow. In the TIPS/DIPS procedure, internal jugular venous access is obtained, and a guidewire is advanced into the IVC. A metallic cannula is placed at the hepatic vein ostium and directed toward the right portal vein using a puncture needle. After successful portal vein puncture, a stiff guidewire is advanced into the splenic vein/superior mesenteric vein, followed by dilation of the parenchymal track and deployment of a covered DIPS stent.

VRT image showing the TIPS stent in a patients with acute Budd Chiari Syndrome

In conclusion, accurate diagnosis and management of BCS rely on imaging modalities due to the rarity of biopsies and the failure of medical treatment in most cases. Imaging findings aid in distinguishing between acute and chronic cases, guiding treatment decisions. Radiological interventions, including angioplasty and stenting, are effective in the majority of cases, with TIPS/DIPS procedures reserved for cases where angioplasty fails or technically not feasible.

SEQUEL FOR PAPER PRESENTATION

S No.	NAME	PAPER TOPIC
1	Dr Harish Shivprasad Gupta	Role of B mode ultra-sonography and sonoelastography in differentiation of benign and malignant cervical lymph node and its histopathological correlation in a tertiary care centre of east India .
2	Dr Soumik Pal	A cross sectional study on role of shear wave elastography in evaluation of chronic liver disease and its correlation with liver function test in a tertiary care centre in Ranchi , Jharkhand .
3	Dr Riya Agarwal	A cross sectional study on assessment of transcranial ultrasound as a diagnostic tool for hypoxic ischemic encephalopathy (HIE) in preterm neonate born at a tertiary care centre in Ranchi , Jharkhand .
4	Dr Mohd. Ismail	Elastographic evaluation (Acoustic radiation force impulse) for differentiation of benign from malignant liver lesions with its histopathological correlation .
5	Dr Manisha Oraon	Radiological normogram of renal cortical elasticity using dynamic shear wave elastography in patients undergoing whole abdomen ultrasound at a tertiary care centre , Jharkhand .
6	Dr Md Shahrukh	To evaluate the role of sonoelastography in differentiating between benign and malignant thyroid nodules and its histopathological correlations.
7	Dr Sonali Priyadarshini Reddy	To evaluate the role of elastography in evaluation of breast lesion and histopathological correlation at a tertiary care centre in Ranchi, Jharkhand.
8	Dr Davidson Shandilya	Spectrum of radiological findings in ultrasound of thyroid nodules.
9	Dr Anil Reddy	Spectrum of radiological findings in ultrasound of benign lesions of the breast with mammographic correlation .
10	Dr Roopshree Bode	Spectrum of radiological findings in benign lesions in female pelvis.
11	Dr Rajshree Ganjeer	Spectrum of radiological finding in USG of benign lesions of the kidneys.

PAPER PRESENTATION - 7TH APRIL 2024

ROLE OF B MODE ULTRA-SONOGRAPHY AND SONOELASTOGRAPHY IN DIFFERENTIATION OF BENIGN & MALIGNANT CERVICAL LYMPH NODE AND ITS HISTOPATHOLOGICAL CORRELATION IN A TERTIARY CARE CENTRE OF EAST INDIA

Dr. Harish Shivprasad Gupta (Junior resident, Department of Radio-diagnosis, RIMS, Ranchi)
Guided by:-Dr. Prof. Suresh Kumar Toppo(H.O.D. Department of Radio-diagnosis, RIMS, Ranchi)

ABSTRACT

Aim:- To determine the effectiveness of B Mode Ultrasonography, Colour Doppler Imaging and Sonoelastography (Shear Wave Elastography) in differentiation of benign and malignant cervical lymph-node with its histopathological correlation

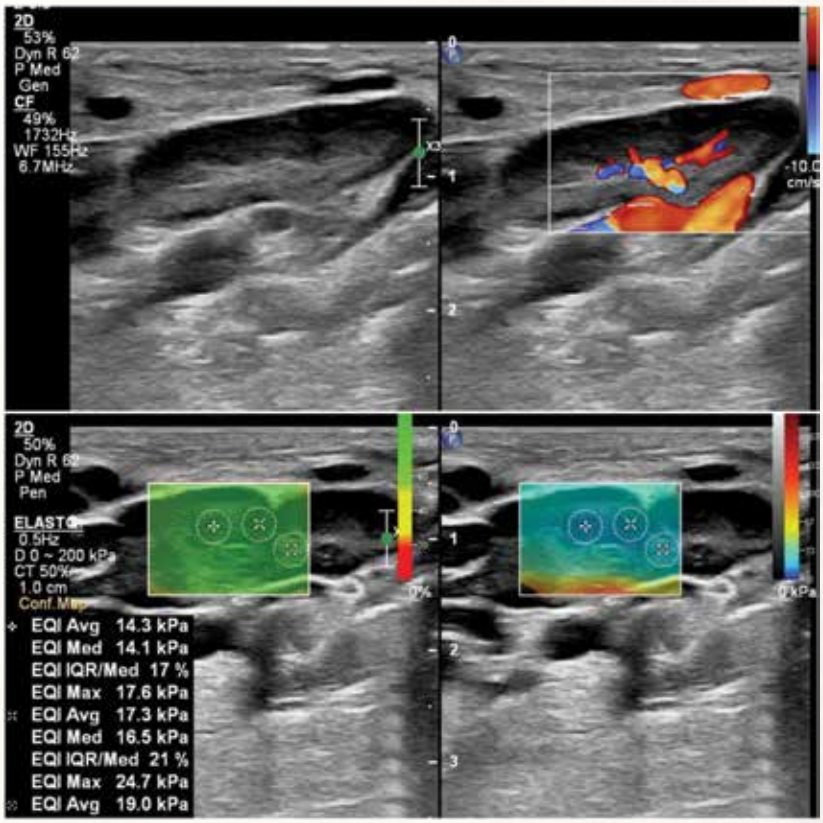

Methodology:- This cross-sectional study was conducted to investigate cervical lymphadenopathy in patients at Department of Radiology, Rajendra Institute of Medical Sciences, Ranchi. Eligible patients were those clinically or via imaging diagnosed with cervical lymphadenopathy, undergoing subsequent lymph node biopsy/FNAC or surgery. 43 samples were evaluated in this study till date of which 3 patients haven't undergone HPE examination were excluded. Imaging procedures utilized B Mode Ultrasonography, Colour Doppler Imaging, and Shear wave Sonoelastography. Data collection involved patient preparation and various ultrasound examinations assessing lymph node characteristics. Histopathological examination post-excision/ biopsy / FNAC determined final diagnoses.

Results:- The combined use of Ultrasonography, Colour Doppler imaging and Sonoelastography yielded better sensitivity (90%), specificity (88%), and diagnostic accuracy (89%) than individual parameters. Of all the above parameters fatty hilum exhibited the highest diagnostic accuracy (73%), followed by vascularity pattern (70%) in ultrasonography, The sensitivity, specificity, and accuracy of elastography alone were 81%, 78%, and 79%, respectively.

Conclusion:- Addition of Sonoelastography showed improved diagnostic accuracy to differentiate between and malignant cervical lymph nodes as compared to Ultrasonography, Colour Doppler imaging or Sonoelastography alone.

A CROSS SECTIONAL STUDY ON ROLE OF SHEAR WAVE ELASTOGRAPHY IN EVALUATION OF CHRONIC LIVER DISEASE AND ITS CORRELATION WITH LIVER FUNCTION TEST IN A TERTIARY CARE CENTRE IN RANCHI, JHARKHAND

Dr Soumik Pal Junior Resident
Dept Of Radio-Diagnosis, RIMS, Ranchi
Guided By : Dr Rajeev Kumar Ranjan Associate Professor Dept of Radio-Diagnosis RIMS, Ranchi

ABSTRACT

Aim: In this study, the elastographic values of liver stiffness is assessed for predicting different stages of liver fibrosis, and to determine the level of agreement between shear wave elastography and serum fibrosis markers.

Methodology: A descriptive, cross-sectional study was performed at the Department of Radiology , Rajendra Institute of Medical Sciences , Ranchi . 46 patients (34 males and 12 females) were evaluated presenting with Chronic liver disease . Elastographic colour maps from different segments of liver were assessed and average stiffness(Kpa) was calculated .

According to stiffness staging of liver fibrosis was done and correlated with fibrosis markers which were calculated from LFT (APRI & FIB-4)

Results: Among the 46 enrolled 170 patients, None were F0-F1, 12 were F2, 26 were F3 , 4 were F4 . 4 patients could not be evaluated due to poor acoustic window . SWE sensitivity and specificity were respectively 85.1% and 82.7% (≥ F2), 88.9% and 90.3% (≥ F3), 93.3% and 98.3% (F4). APRI and FIB-4 values moderately correlated with stiffness values and staging (APRI : Sn72% Sp 70% , FIB-4 Sn 78% Sp 73% for F4)

Conclusion: SWE showed a significant correlation with the severity of liver fibrosis and was useful and accurate to predict significant and advanced fibrosis, comparable with serum markers.

A CROSS SECTIONAL STUDY ON ASSESSMENT OF TRANSCRANIAL ULTRASOUND AS A DIAGNOSTIC TOOL FOR HYPOXIC ISCHEMIC ENCEPHALOPATHY (HIE) IN PRETERM NEONATE BORN AT A TERTIARY CARE CENTRE IN RANCHI, JHARKHAND

Presenting author: Dr. Riya Agarwal (JRII, Department of Radiodiagnosis, RIMS, Ranchi)
Co-authors: Dr. Suresh Kumar Toppo (Professor and HOD, Department of Radiodiagnosis, RIMS, Ranchi)
Dr Nisha Rai (Assistant Professor, Department of Radiodiagnosis, RIMS, Ranchi)
Affiliations: Department of Radiodiagnosis, RIMS, Ranchi

Objective: To access the importance of transcranial ultrasound as an investigatory modality for diagnosing HIE in preterm neonates and also to determine its diagnostic accuracy.

Materials and Methods: This is a single centre cross sectional study in which transcranial USG of preterm neonates suspected of HIE, and born in RIMS was performed. Till now we have included 20 such patients. The results are tabulated under major clinical features (like delayed cry, birth weight, mode of delivery, seizures) and was correlated with the transcranial USG findings.

Results: The mean age of the patients studied was 2 days (1-4 days), with most common clinical feature being low birth weight (75%), followed by delayed cry in 45% neonates and seizures in 40% of them. Also, 40% of the neonates were born by LSCS. On transcranial USG, we found positive findings of germinal matrix haemorrhage, sub ependymal cysts and sub cortical cysts in 20% of the patients. Also, 1 patient was diagnosed with posterior fossa malformation.

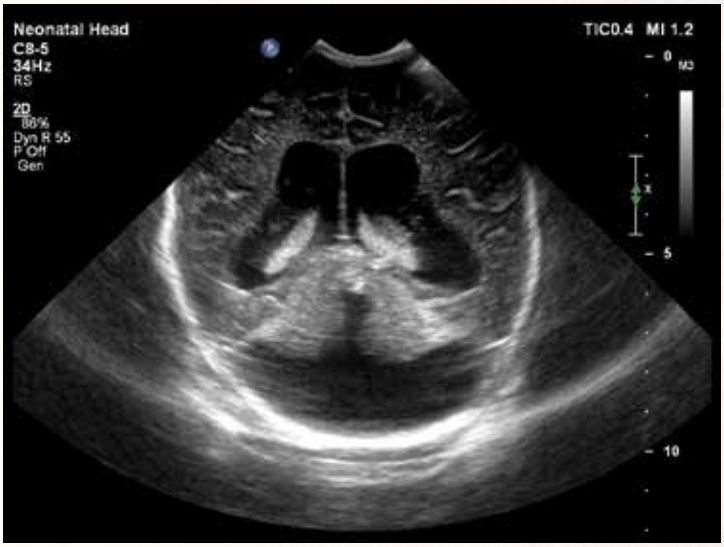

Conclusion: Transcranial USG is a simple, affordable and non-invasive procedure that can be conducted soon after birth. It can be repeated as and when required, allowing for continuous monitoring of brain development and progression of brain injuries. Hence, it can aid in early intervention and prevent further complications.

ELASTOGRAPHIC EVALUATION (ACOUSTIC RADIATION FORCE IMPULSE) FOR DIFFERENTIATION OF BENIGN FROM MALIGNANT LIVER LESIONS WITH ITS HISTOPATHOLOGICAL CORRELATION

Dr. Mohd Ismail Junior Resident, Department of Radio-diagnosis RIMS, Ranchi
Guided by : Dr. Anima Ranjni Xalxo Assistant Professor Department of Radio-diagnosis RIMS, Ranchi.

ABSTRACT

Background: Accurate differentiation of benign and malignant liver lesions is crucial for optimal patient management. Elastography, specifically Acoustic Radiation Force Impulse (ARFI), has emerged as a promising non-invasive tool for this purpose.

Methods: We conducted a retrospective study involving patients with liver lesions who underwent ARFI elastography followed by histopathological examination.

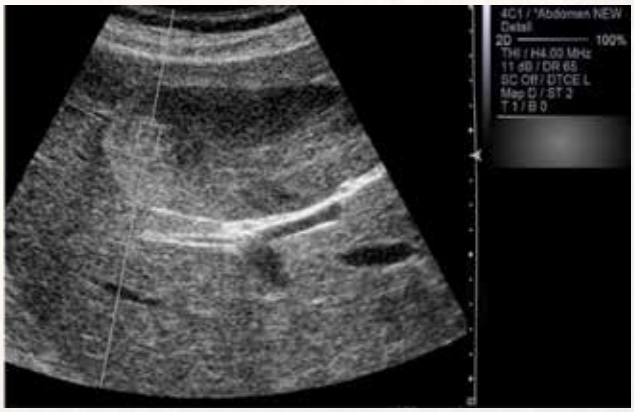

Lesion stiffness was measured using ARFI, and the results were correlated with histopathological findings to assess the diagnostic accuracy of ARFI elastography.

Results: A total of 40 patients with liver lesions were included in the study. ARFI elastography demonstrated a significant difference in tissue stiffness between benign and malignant lesions ($p < 0.001$). The mean stiffness values for benign lesions were 1.56±0.31m/s, whereas for malignant lesions, the mean stiffness was 2.65±0.45m/s. Using a cutoff value of 2m/s, ARFI elastography achieved a sensitivity of 95%, specificity of 95%, and accuracy of 95% in discriminating benign from malignant liver lesions. Histopathological correlation confirmed the accuracy of ARFI elastography findings.

Conclusion: ARFI elastography is a valuable non-invasive tool for differentiating between benign and malignant liver lesions, with high diagnostic accuracy. Its integration into routine clinical practice can aid in better patient management and treatment decisions.

RADIOLOGICAL NORMOGRAM OF RENAL CORTICAL ELASTICITY USING DYNAMIC SHEAR WAVE ELASTOGRAPHY IN PATIENTS UNDERGOING WHOLE ABDOMEN ULTRASOUND AT A TERTIARY CARE CENTRE, JHARKHAND

Dr Manisha Oraon
Junior Resident (Academic) MD Radiodiagnosis RIMS, Ranchi
Guided by : Dr. Suresh Kumar Toppo Head of Department Department of Radio Diagnosis RIMS Ranchi

ABSTRACT

Background: Elastography has emerged as a promising tool for assessing tissue elasticity, including renal cortical tissue. Renal shear wave elastography has the potential to assess early renal damage. Hence, it is important to assess the normal values of elasticity using shear wave elastography. The primary objective of this study is to establish the normogram of renal cortical elasticity and hence, we can use these values as baseline or reference values to assess the progression of renal disease in patients especially CKD, diabetics and hypertensives in near future.

Methods: Cross sectional study was conducted to establish the normogram of renal cortical elasticity using dynamic shear wave elastography and to establish the influence of factors affecting the renal cortical elasticity. Statistical analysis was performed to establish to establish the influence of factors affecting the renal cortical elasticity.

Results: The study established normative values for renal cortical elasticity using dynamic shear wave USG elastography, demonstrating variations across age groups, sexes and kidney profile. The multiple regression analysis of the right kidney showed a statistically significant influence of BMI (p-value 0.002), width (p-value 0.049) and parenchymal thickness (p-value 0.012) on renal cortical elasticity. However, no statistically significant influence of age, gender, length, cortical thickness and skin to cortex distance on renal elasticity established. The Multiple regression analysis of the left kidney showed a statistically significant influence of BMI on renal elasticity (p-value 0.041). However, no statistical significance noted between age, gender, length, width, parenchymal thickness, cortical thickness and skin to cortex distance. Overall, the normogram provides a reference range for renal cortical elasticity in healthy individuals, facilitating the interpretation of elastography findings in clinical practice.

Conclusion: The normal renal cortical shear wave elasticity of kidney was established. We found that elasticity measured in terms of shear wave velocity is independent of age, gender, length and cortical thickness. We also found a negative correlation between shear wave velocity and BMI in both kidneys. This study provides reference values which can be used for future clinical applications of elastography of the normal kidney. Further studies should be conducted in the future by taking into account the effect of renal perfusion also. Future studies in

patients with renal diseases would help in assessing if renal cortical shear wave velocity can be used as a non-invasive biomarker of renal disease.

TO EVALUATE THE ROLE OF SONOELASTOGRAPHY IN DIFFERENTIATING BETWEEN BENIGN AND MALIGNANT THYROID NODULES AND ITS HISTOPATHOLOGICAL CORRELATIONS

Dr. Md Shahrukh Junior Resident
Dept. of Radio-Diagnosis, RIMS, Ranchi
Guided By: Dr. Suresh Kumar Toppo Professor & Hod, Dept. of Radiodiagnosis, RIMS, Ranchi

ABSTRACT

Purpose: To evaluate the role of sonoelastography in differentiating between benign and malignant thyroid nodules and its histopathological correlations

Methods: This prospective study was performed in dept of Radiodiagnosis, RIMS, Ranchi. 48 patients (15 males and 33 females) were evaluated presenting with thyroid nodules. The age range of the patients was 15-60 yrs. All included patients received either cytology using FNAB and/or histology from thyroid surgery to verify the diagnosis. Elastographic maps (color coding) and thyroid stiffness index were calculated for all nodules.

Results: Malignant nodules had a higher degree of color and strain ratio compared to benign nodules, with a statistically significant difference ($p < 0.05$). Nodules with an elastography score of ≤2.8 were benign, while those with an elastography score of 3 and 4 were mostly malignant. The sensitivity and specificity of the US- elastography for differentiating between benign and malignant thyroid nodules were 90.9% and 97.3% respectively.

Conclusion: Sonoelastography of thyroid nodules was assessed as a complementary diagnostic tool to thyroid ultrasound to further characterize the probable nature of the nodule. ARFI elastography provides new set of information that is not based on the anatomical features but on the relative elasticity of the lesion and hence becomes complementary to the ultrasound features. It is more sensitive and specific than ultrasound in differentiating benign and malignant thyroid nodules, but cannot be used in isolation for diagnosis of thyroid nodules.

TO EVALUATE THE ROLE OF ELASTOGRAPHY IN EVALUATION OF BREAST LESION AND HISTOPATHOLOGICAL CORRELATION AT A TERTIARY CARE CENTRE IN RANCHI, JHARKHAND

Dr Sonali Priyadarsini Reddy,
Junior Resident, Dept. of Radiodiagnosis, RIMS, Ranchi
Guided By : Dr Rajeev Kumar Ranjan, Associate Professor, Dept. of Radiodiagnosis, Rims, Ranchi

ABSTRACT

Purpose - To evaluate the role of Elastography in evaluation of breast lesion and histopathological correlation at a tertiary care centre in Ranchi, Jharkhand.

Methods - The cross sectional study was performed in Dept. of Radiodiagnosis, RIMS, Ranchi. 50 patients were evaluated presenting with breast lesions. Out of 50 patients, 25 patients were with benign breast lesions and other 25 patients were with malignant breast lesions proven by histopathological examination. Elastographic maps (Colour coding) and tissue stiffness indices were calculated.

Results - All elastographic score 1 lesions were benign whereas all score 5 lesions were malignant.

Out of 23 lesions with elastographic score 2 or 3, 5 were histologically malignant (False negative). Out of 13 lesions with elastographic score 4, 5 were histologically benign (False positive).

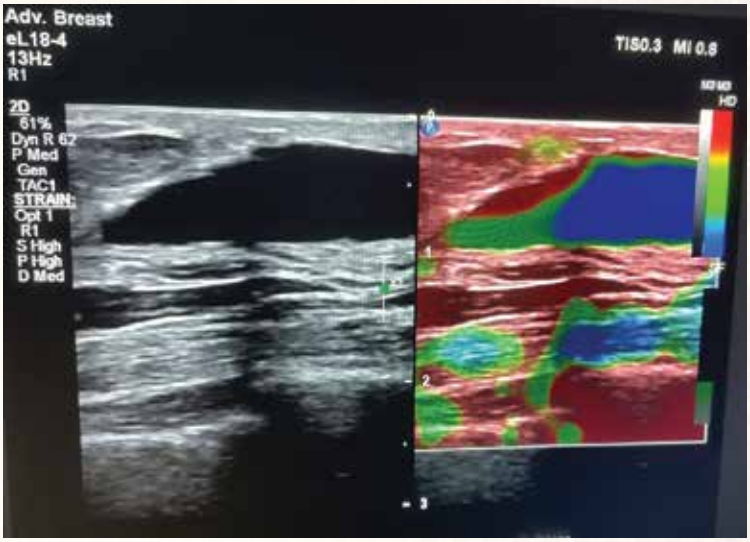

Considering scores of 1 to 3 are benign and 4 and 5 as malignant, Elastography had sensitivity of 62.5%, specificity of 91%, a PPV of 83.3% and a NPV of 76.9%.

Conclusion – Elastography is a fast, easy, non-invasive technique when used as a complimentary technique in addition to B mode sonography.

It increases the diagnostic specificity for characterization of breast lesions.

Thus elasticity helps in reducing unnecessary biopsy and false positive rate and thereby reduces mortality.

SEQUEL FOR POSTER PRESENTATION

S.No.	Name	POSTER TOPIC
1	Dr Harsha Kaur	Giant cell tumor of tendon sheath : A case report
2	Dr Arti Kumari	RUPTURED OVARIAN DERMOID CYST : A CASE REPORT
3	Dr Rashmi Kumari	Maduramycosis : A case report
4	Dr Jainesh Toppo	Adenomyosis : A case report
5	Dr Nisha Pandey	Caudal regression syndrome : A case report of a rare congenital anomaly
6	**Dr. Harish Shivprasad Gupta**	Case report: Stanford type A acute Aortic dissection
7	**Dr Soumik Pal**	Imaging Features of Uterine AVM
8	Dr Prakhar Srivastava	A comparative study of cystic hygroma and branchial cyst
9	Dr Akash Rohit Kujur	Desmoid tumor : A case report
10	Dr Ruchi Pandey	Discribe the rare cases of Hypertropic pyloric stenosis in dizygotic twins
11	Dr Simran	Benign fibroosseous lesion of the craniofacial complex likely fibrous dysplasia : A case report
12	Dr Shruti Shree	Case report on posterior fossa mass lesion in a 6 year old boy – Medulloblastoma
13	Dr Sunila Kumari Singh	Imaging finding in case of craniopharyngioma
14	Dr Jayanta Kumar Ghosh	Carotid body tumor : A case report

GIANT CELL TUMOR OF TENDON SEATH : A CASE REPORT

Authors: Dr. Suresh Kumar Toppo, Dr. Rajeev Kumar Ranjan, Dr. Harsha Kaur
Presenting author: Dr. Harsha Kaur

Introduction:

Giant Cell Tumor of tendon seath, also termed as pigmented nodular tenosynovitis. Giant cell tumor of the tendon sheath (GCTTS) is a type of benign soft tissue tumor.

Case Report:

A 64 year old male presented with complains of a **swelling** over the **right index finger**, which was **insidious in onset and gradually progressed** to the current size in a span of **6 months**. The patient attributes this to trivial trauma. Physical exam revealed a **palpable mass with limited range of motion.**

Radiograph of of the right hand showed soft tissue shadow around the proximal phalanx of middle finger with scalloping of the shaft of the proximal phalanx of index finger. There was no bony involvement.

Grey scale ultrasound of the swelling was done with a high frequency linear array transducer (5-12 MHz). It revealed a solid, well circumscribed heteroechoic lesion width approximately 2 cm along the flexor tendon the right index finger or a length of 5 cm, which seems to completely envelop the flexor tendon with internal vascularity on colour doppler. The lesion also extended into the palm along the same tendon sheath.

MRI of hand revealed T1 hypointense and T2 hyperintense lobulated soft tissue density masses along the flexor tendon the right index finger. The lesion seemed to completely envelop the flexor tendon sheath.

FNAC confirmed of Pigmented Villonodular Synovitis.

Conclusion: Giant cell tumor of the tendon sheath (GCTTS) is a type of benign soft tissue tumor. The World Health Organization distinguishes between two types of giant cell lesions originating from the tendon and the synovium. GCTTS can be classified as localized (L-) or diffuse (D-) type. **L-GCTTS** primarily occurs in the **tendon sheaths of the hand and foot** and exhibits clear boundaries, whereas D-GCTTS occurs in large joints with a more aggressive growth pattern and associated high recurrence rate.




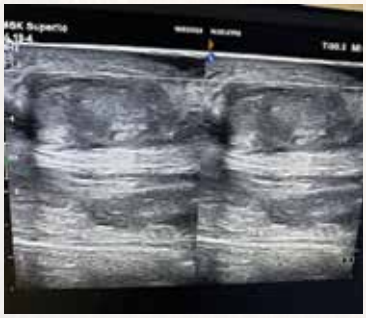


RUPTURED OVARIAN DERMOID CYST : A CASE REPORT

By : Dr Arti Kumari , Junior Resident (3rd year)
Under the guidance of : Dr. Suresh Kumar Toppo (Professor and HOD)
Dr. Rajeev Kumar Ranjan (Associate Professor)
Department of Radiodiagnosis , RIMS RANCHI

CASE REPORT :

A 25 years old, nulliparous, unmarried woman presented with complaints of recurrent chronic pain abdomen since five months with on and off constipation and vomiting. Her medical history was insignificant. She had normal menstrual cycles. Physical examination revealed a globular lump in the pelvis which was slightly tender on palpation. It was associated with mild abdominal rigidity and distension.

TRANS ABDOMINAL ULTRASOUND revealed an echogenic mass showing posterior acoustic shadowing with associated cystic component and few foci of calcification in the pelvis involving both the adnexal region. Both the ovaries could not be delineated separately from the mass. Uterus was normal.

PLAIN AND CONTRAST ENHANCED CT was advised for further evaluation which showed two masses composed of fat and fluid with calcific focus seen within the pelvis. There was surrounding fat stranding. Also a chain of fat density material is seen extending from the left mass along the left anterior abdominal wall. There was sub acute intestinal obstruction with no underlying bowel wall thickening or bowel mass likely due to adhesion band .

Patient underwent exploratory laparotomy which revealed a ruptured dermoid cyst with caseous material and hair follicle. The peritoneal cavity showed signs of inflammation and widespread adherence to anterior abdominal wall. The cyst was adherent to adjacent bowel loops. Adhesiolysis was done. She was managed with dermoid removal and B/l oophorectomy.

MACROSCOPIC DESCRIPTION: showed mass with fatty cut surface with hair tufts

MICROSCOPIC DESCRIPTION : showed mature cystic teratoma which predominantly consists of adnexal structures and skin. No immature elements were seen.

FINAL DIAGNOSIS: typical appearances of a ruptured dermoid cyst with fat density sebaceous material layering in the abdomen.

DISCUSSION :

Mature cystic teratoma is the most common ovarian germ cell tumor composed of skin, hair, tooth and sebum. It can present with complications like torsion, rupture, infection etc. Here we present with a 25years unmarried female who presented with lower abdominal pain, vomiting and rigidity of abdomen. Ultrasonography of the abdomen and pelvis followed by contrast enhanced CT showed the features consistent with a ruptured dermoid cyst. Exploratory laparotomy and histopathological examination of the specimen confirmed the diagnosis. So, following rupture of the dermoid patients may progress to a stage of chronic peritonitis. At this stage, the radiological assessment may be crucial for appropriate diagnosis and further management.


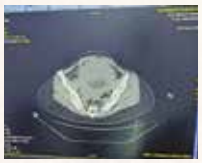
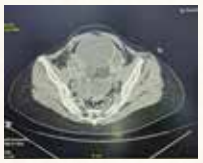
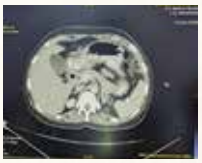
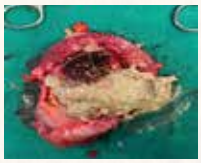


MADURAMYCOSIS : A CASE REPORT

By : Dr Rashmi Kumari , Junior Resident (3rd year)
Under the guidance of :Dr. Suresh Kumar Toppo (Professor and HOD)
Dr. Rajeev Kumar Ranjan (Associate Professor)
Department of Radiodiagnosis

CASE REPORT :

A 40-year-old farmer presented with a painless swelling on the dorsum of his right foot, which had been gradually increasing in size over the past six months. There was h/o prick injury with vegetative matter. Clinical examination revealed sinus tracts with scanty discharge containing granules. Radiological investigations, including X-ray, ultrasound, and MRI, were performed to evaluate the extent of the lesion and aid in diagnosis.

X-ray imaging showed soft tissue mass with focal areas of rarefaction ,lysis and sclerosis of the underlying bone, while ultrasound revealed hypoechoic areas with internal echoes representing grain-like structures.

MRI demonstrated extensive soft tissue involvement and bone destruction, confirming the diagnosis of Madura foot with **Dot in a circle sign** which is classic appearance on T2 weighted images which show a small rounded hyperintensity (representing granulation tissue), surrounded by a low signal intensity rim (representing fibrous septa) with a hypointense dot (representing susceptibility loss due to fungi) in the center

Discussion:

The radiological findings in Madura foot typically include bone involvement with features such as osteolysis, periosteal reaction, and soft tissue calcifications. Ultrasound is useful for detecting the presence of grain-like structures within the soft tissues. MRI provides detailed information about the extent of soft tissue involvement and aids in surgical planning. . Recognizing the characteristic radiological features of Madura foot is essential for accurate diagnosis and timely initiation of appropriate treatment, which typically involves a combination of antifungal agents and surgical debridement.

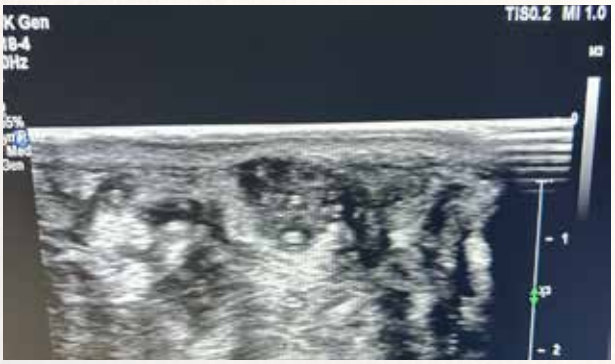

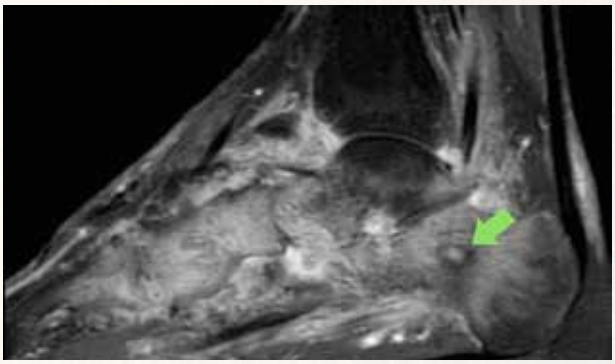

ADENOMYOSIS : A CASE REPORT

By : Dr Jainesh Toppo , Junior Resident (3rd year)
Under guidance of : Dr. Suresh Kumar Toppo (HOD , Professor)
Department of Radiodiagnosis.

CASE REPORT: We present the case of a 53-year-old woman who presented with complaints of severe dysmenorrhea, menorrhagia since one and a half weeks , she had similar complains for the past two years. Her medical history was significant for four uncomplicated vaginal deliveries and regular menstrual cycles. Physical examination revealed enlarged, firm and tender uterus on palpation.

Transabdominal and Transvaginal ultrasound (TVUS) demonstrated a globally enlarged uterus with heterogeneous myometrial echotexture and multiple small cystic spaces giving fan shaped shadowing suggestive of adenomyosis. The patient was counseled regarding surgical intervention with hysterectomy as her family was complete. Fan shaped shadowing and trans-lesional vascularity suggestive of Adenomyosis .

CECT Abdomen and Pelvis : Well defined globular enlarged uterus .

Post Operative : globular enlarged uterus with thickened and spongy appearing myometrial wall .

On HPE –there was presence of ectopic endometrial glandular and stromal tissue within the myometrium -the features were suggestive of adenomyosis .

DISCUSSION :

Adenomyosis is a common condition characterized by invasion of glands and stroma within the myometrium This results in myometrial hypertrophy and hyperplasia around the ectopic endometrial glands. It typically presents with symptoms such as dysmenorrhea, menorrhagia, symmetrically enlarged tender and pelvic pain, leading to significant morbidity among affected individuals. Here, we present a case report of a 53-year-old female with symptomatic adenomyosis, highlighting the clinical presentation, radiological findings(Ultrasonographic findings on the basis of MUSA consensus), and management approach.

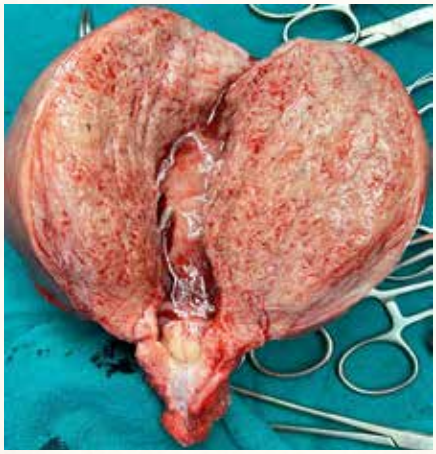

CAUDAL REGRESSION SYNDROME: A CASE REPORT OF A RARE CONGENITAL ANOMALY

Authors: Dr Nisha Pandey, Dr Suresh Kumar Toppo
Presenting author: Dr Nisha Pandey
Affiliations: Department of Radiodiagnosis & Imaging, RIMS Ranchi

Introduction:

Caudal Regression syndrome is a rare congenital abnormality resulting from a developmental failure of a segment of vertebral column and spinal cord. Maternal hyperglycemia is the most important recognised teratogen. Caudal regression syndrome occurs in upto 1% of pregnancies of diabetic mothers. Severe forms can cause early neonatal death as well.

Case Presentation:

A 15 year old child with a long history of lower extremity weakness and parasthesia ,presented with worsening lower back pain and left iliac fossa pain along with irregular menstrual cycle. The patient underwent MRI LS spine which demonstrated sacrococcygeal hypoplasia , including absent S2-S5 and coccygeal segments with hypoplastic S1 segment. The conus medullaris is elongated and tethered by a fatty filum terminale. MRI and USG abdomen demonstrated bicornuate unicollis uterus with a left adnexal haemorrhagic cyst, right renal agenesis and left hydroureteronephrosis. The patient had a previous history of anorectal malformation which was operated.

Discussion:

Caudal Regression Syndrome results from an abnormal development of caudal aspect of spinal cord and vertebral column. The majority of cases are sporadic with few having genetic contribution. Clinically patient presents with a wide range of symptoms like motor and sensory disturbances, gastrointestinal, skeletal and genitourinary problems.

Conclusion :

A diagnostic algorithm for CRS is crucial to understand the types of CRS and assist radiologists and clinicians in managing patients, to avoid unnecessary examinations, radiation, and improve the patient's quality of life.

CASE REPORT: STANFORD TYPE A ACUTE AORTIC DISSECTION

Dr. Harish Shivprasad Gupta (Junior resident, Department of Radio-diagnosis, RIMS, Ranchi)
Guided by:-Dr. Prof. Suresh Kumar Toppo(H.O.D. Department of Radio-diagnosis, RIMS, Ranchi)
Dr. Rajeev Kumar Ranjan(Associate Professor Department of Radio-diagnosis, RIMS, Ranchi)

ABSTRACT

Introduction

Aortic dissection, the most common acute aortic emergency, happens 2–3 times more often than acute rupture of an aortic aneurysm. It typically occurs more frequently in men during their 6th and 7th decades of life. The initial event is a tear in the intima which allows blood to enter the aortic wall creating a true and false lumen.

Case presentation

35 year old male came to the emergency department with history of sudden onset, sharp, severe chest pain typically radiating to back associated with increased sweating and difficulty in breathing. Clinical examination showed raised blood pressure and diastolic murmur on chest auscultation. The patient underwent chest x-ray, ECG and echocardiography with initial diagnosis of acute coronary syndrome. Echocardiography shows dilated ascending aorta with intimal flap in its lumen. Further evaluation with CT angiography of aorta was done which demonstrated dilatation of ascending aorta with an intimal flap in its lumen suggesting Stanford type A aortic dissection with aneurysmal dilatation of ascending aorta. The patient then underwent open surgery with aortic stent placement.

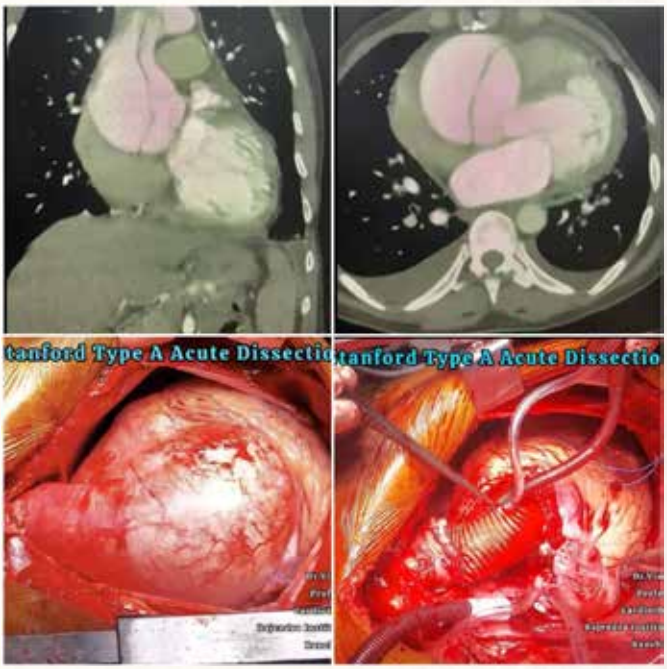

Discussion

Prognosis of aortic dissection is poor, with 20% of patients dying before they reach hospital. The mortality for type A dissection is higher than for type B. The symptom complex overlap with many other potential diagnosis (e.g. Myocardial infarction) and cross-sectional imaging is essential to confirm the diagnosis and look for other complications.

Conclusion:-

CT has become imaging modality of choice in aortic dissection with it wide availability and fast acquisition which become instrumental in diagnosis, intervention planning and prognosis of the patient.

IMAGING FEATURES OF UTERINE AVM

Dr Soumik Pal (Junior Resident, Department of Radio-Diagnosis, RIMS , Ranchi Guided by –
Dr Rajeev Kumar Ranjan(Associate Professor, Department of Radio-Diagnosis, RIMS , Ranchi)
Dr Prof Suresh Kumar Toppo (HOD , Department of Radio-Diagnosis, RIMS , Ranchi)

ABSTRACT

Introduction

Uterine arteriovenous malformation (AVM) is a rare vascular condition , characterised by dilatation of the intervillous space deep inside the myometrium, allowing a direct flow from the arterial system towards the venous system, without participation of capillary vessels. Such condition consists of about 1-2% of all genital and intraperitoneal hemorrhages.

Case Presentation

27yr old female who was diagnosed with partial molar pregnancy had undergone D&C for the same 6 months back . At present , patient presented with bleeding p/v and mild lower abdominal pain .Patient underwent Ultrasound lower abdomen followed by subsequent CT and MRI . Ultrasound showed multiple tortous intramural vessels and a large nidus within posterior myometrium . Feeding vasculature was identified in subsequent CT and Multiple serpentine flow void were identified in MRI . Patient was sent to Obs & gynae Department for subsequent management .

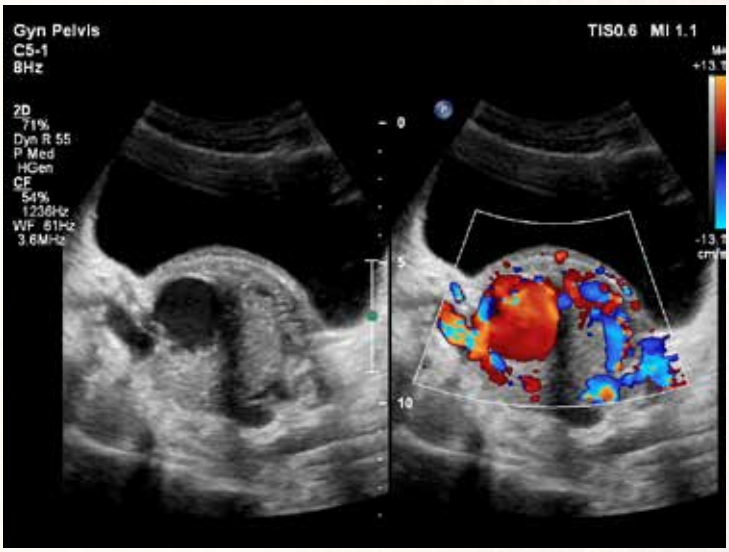

Discussion

Uterine AVMs may be either congenital or acquired. The congenital presentation is rare, resulting from abnormal development of the primitive vascular structures. However, in most cases such malformation is acquired, with a great variety of causes, including gestational trophoblastic disease (GTD), pelvic trauma, surgical procedures (cesarean section, curettage), cervical or endometrial carcinoma, infection and exposure to diethylstilbestrol. Historically, the diagnosis was made after laparotomy. Subsequently, angiography became the gold standard.

Conclusion

Currently, Transabdominal and transvaginal Doppler US is the most utilized method to diagnose Uterine AVM. CT Angiography is reserved for patients submitted to surgical treatment or therapeutic embolization to identify the feeding vessels .

A COMPARATIVE STUDY OF BRACHIAL CYST AND CYSTIC HYGROMA

Presenting Author: Dr. Prakhar Srivastava
Co- authors: Dr. Suresh Kumar Toppo (Professor and Head of Department)
Dr. Rajeev Kumar Ranjan (Associate professor)
Affiliations: Department of Radiodiagnosis, RIMS, Ranchi

Case presentation:

Cystic Hygroma:

A 2-month-old male infant is brought to the pediatrician's office by his parents due to the Presence of a mass in the left side of his neck. The parents report that they first noticed the Mass shortly after birth, and it has been gradually increasing in size. The infant is otherwise Healthy with no significant medical history. On physical examination, a soft, cystic mass is Palpated in the left cervical region. The mass is non-tender and mobile, measuring Approximately 3 cm in diameter. There are no signs of inflammation or infection.

USG: Ultrasound examination of the neck reveals a well-defined, cystic lesion measuring approximately [size 75 x 50 mm] located in the left neck region. The lesion appears to be predominantly anechoic with thin septations and no internal vascularity noted on color Doppler imaging. The cystic structure demonstrates posterior acoustic enhancement. There is no evidence of invasion into surrounding structures.

CT: Large simple fluid density cystic lesion of size approx 75x50x72mm (volume approx 132ml) noted in the posterior triangle of left neck, posterior to sternocleidomastoid and lateral to carotid vessel. The lesion extends inferiorly till transverse process of C7 vertebrae. Few thin septations seen within it. No calcification or solid components noted. No abnormal enhancement seen. F/S/O-Macrocystic lymphatic malformation (Cystic Hygroma)

Branchial cyst: 25-year-old female presented to the radiology department with a chief complaint of a painless swelling in the left lateral neck region for the past six months. The patient reported gradual enlargement of the swelling with no associated symptoms such as pain, dysphagia, or dyspnea. There was no history of trauma or previous surgeries in the neck region.

USG: Ultrasound examination of the neck reveals few (3-4) hypoechoic nodular lesion largest one of About 24.7 x 16.8 mm seen in left submandibular Region, having hilar vascularity.

CT: 3.5 X 2.1 X 2.8 cms, Thin walled, well capsulated, nonenhancing cystic lesion in the left mid neck, perimandibular in location along the myofascial planes, antero-medial to left sterno-cleido-mastoid muscle .

Conclusion:

In conclusion, distinguishing between cystic hygroma and branchial cysts based on radiological findings is crucial for accurate diagnosis and appropriate management. While both lesions typically present as cystic masses in the neck region, careful assessment of location, shape, wall thickness, contents, enhancement pattern, association with lymphadenopathy, and differential diagnosis aids in differentiation.

Cystic hygromas tend to involve the cervical lymphatic chain, exhibit multiloculated configurations, and may be associated with lymphadenopathy, while branchial cysts are commonly located along the anterior border of the sternocleidomastoid muscle and present as unilocular or multilocular cysts with smooth walls. However, histopathological examination remains the gold standard for definitive diagnosis, necessitating a multidisciplinary approach involving radiologists, clinicians, and pathologists for optimal patient care.

DESMOID TUMOR – A CASE REPORT

BY Dr AKASH ROHIT KUJUR , JUNIOR RESIDENT (1st year)
Under the guidance of : Dr Suresh Kumar Toppo (Head of Department)
Dr Rajeev Kumar Ranjan (Associate Professor)
Affiliations: Department of Radiodiagnosis , RIMS Ranchi

Introduction :

Desmoid tumors are benign and non inflammatory fibroblastic tumors with a tendency for local invasion and recurrence but without metastasis . Epidemiology – Most common in age between 20 to 40 years . Male : Female predilection – 2:1 . Associated with Pregnancy , Estrogen therapy and Gardner syndrome . Frequently occurs in abdominal wall , root of mesentry and retroperitoneum .

Case Presentation :

This 39 year old female presented with complaint of swelling in left inguinal region since a duration of 1 year . The swelling was associated with pain which was sudden in onset , dull aching in nature and radiating to left upper thigh region . The patient underwent CT whole abdomen which demonstrated a well circumscribed round to oval mass lesion measuring approx. 38x64x49 mm was noted in the intramuscular plane of left lower anterior abdominal wall . Heterogenous enhancement of the lesion was noted following administration of intravenous contrast . USG whole abdomen demonstrated an ovoid shape heterogeneously hypoechoic lesion of size approx. 85 x 41 mm noted in left rectus abdominis muscle . Lesion was buldging into overlying suncutaneous plane and underlying peritoneum .

Intra operative findings :

A mass of size approx. 7 x 5 cm , firm , adhered to anterior abdominal wall and peritoneum was noted .


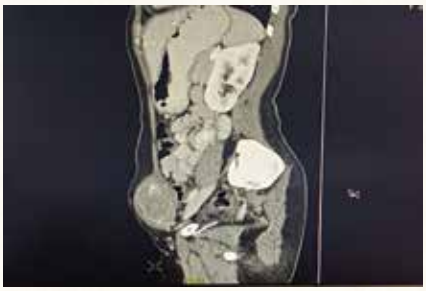
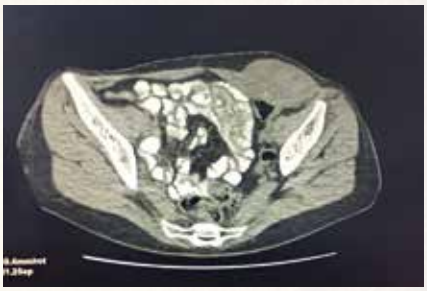

Histology :

Biopsy specimen confirmed the diagnosis characterized by long sweeping fascicles with thin walled vessels and hemorrhages were noted .

Conclusion :

In summary , desmoid tumors represent a rare entity characterized by their locally aggressive nature and propensity for infiltration into surrounding tissues . Most of the asymptomatic cases have good prognosis while management options for symptomatic cases include surgical resection and radiotherapy .

TO DESCRIBE THE RARE CASE OF HYPERTROPHIC PYLORIC STENOSIS IN DIZYGOTIC TWINS

Presenting author: Dr Ruchi Pandey
Co- authors- Dr Suresh Kumar Toppo, Dr Nisha Rai Affiliations: Department of Radiodiagnosis , Rims, Ranchi

Introduction:

Infantile hypertrophic pyloric stenosis (IHPS) is a disorder encountered in infancy that is caused by hypertrophy of the musculature of the pylorus of the stomach. It may present as partial or complete gastric outlet obstruction. Multiple previous literatures have discussed the incidences and variability in the presentation of IHPS. However, there are very few reports of IHPS occurring in dizygotic twins, especially dizygotic twins of different sexes.

Case presentation:

Dizygotic twins, 'Twin A' and 'Twin B' of opposite sex born in our facility at 36+1 weeks of gestation to a 24- year-old G3P1L1 female with gestational diabetes mellitus well controlled on diet presented to our Rims emergency department at two and four weeks of life respectively with non-bilious vomiting after each feeding.

USG findings

The pylorus shows thickened muscle layer measures about 5.3 mm in thickness, it is also elongated and measures 21 mm in length. This is indicative of hypertrophic pyloric stenosis

The cervix sign of pyloric stenosis describes the indentation of the pylorus into the fluid-filled antrum, seen in pyloric stenosis

The target sign of pyloric stenosis is a sign seen due to hypertrophied hypoechoic muscle surrounding echogenic mucosa

As seen in Twin A Discussion:

Some features related to IHPS with regards to previous literature points towards hereditary patterns like male preponderance and increased occurrence among monozygotic twins and similar occurrence in dizygotic twins . However, no specific autosomal or recessive pattern of inheritance has ever been observed in the occurrence of IHPS.

Conclusion:

In conclusion, the case presentation of infantile hypertrophic pyloric stenosis (IHPS) in dizygotic twins of opposite sexes underscores the rarity of this occurrence. While IHPS typically presents with certain characteristic features such as non-bilious vomiting and palpable abdominal mass, its occurrence in twins adds complexity to its etiology. Although previous literature suggests a hereditary component in IHPS, including a male preponderance and occurrences in both monozygotic and dizygotic twins, the specific genetic mechanisms remain elusive. This

case highlights the importance of considering IHPS in the differential diagnosis of neonatal vomiting, especially in twins with a positive family history, and emphasizes the need for further research to elucidate its genetic underpinnings.

TO DESCRIBE BENIGN FIBROOSSEOUS LESION OF THE CRANIOFACIAL COMPLEX IN A 17 YEAR MALE LIKELY FIBROUS DYSPLASIA: A CASE REPORT

Presenting Author: Dr. Simran
Under the guidance of : Dr suresh Kumar Toppo (Professor,HOD) , Dr. Rajeev Kumar Ranjan(Associate professor) .
Affiliations: Department of Radiodiagnosis, RIMS, Ranchi

Introduction:

Fibrous dysplasia (FD) is a developmental benign medullary fibro-osseous process characterized by the failure to form mature lamellar bone and arrest as woven bone that can be multifocal. It can affect any bone and occur in a monostotic form involving only one bone or a polyostotic form involving multiple bones. In McCune-Albright syndrome (MAS), fibrous dysplasia is associated with hyperfunction of endocrine organs and overproduction of melanin in the skin, while Mazabraud syndrome FD is associated with intramuscular myxomas.

Case presentation:

This is 17 years old boy presented with complains of painless swelling on the left frontal and parietal bone facial deformity and nasal stuffiness since 2 years .

On CT scan there was extensive bony expansion with cortical destruction and areas of heterogeneous bone density ranging from sclerotic to lucent in the right and left parietal bone,left frontal bone squamous and mastoid part of left temporal bone, sphenoid sinus, clivus, lesser and greater wing of sphenoid, walls of left maxillary sinus . The majority of the affected bones demonstrated a ground glass appearance.

An incisional biopsy was obtained and microscopic examination showed irregular bony trabeculae in Chinese script pattern scattered within fibrous stroma.

Discussion:

Radiological evaluation, particularly CT scan, which better delineates morphological changes in bone is the modality of choice. CT defines the anatomy of individual lesions and establishes the extent of disease. CT scans may identify soft tissue masses, bone destruction and suggest malignant transformation. Treatment of the disease is mainly palliative, focusing on optimising function and minimising morbidity related to deformities and fractures. Antiresorptive therapy with bisphosphonates has been advocated due to high levels of bone resorbtion frequently seen in FD tissue. The typical asymptomatic lesion, which is identified incidentally, requires the follow-up with

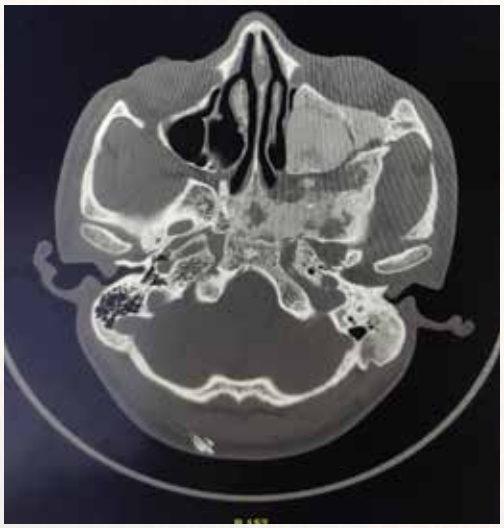

serial radiographs to confirm that the lesion is biologically inactive and mechanically insignificant. Symptomatic or atypical lesions may require surgical excision for histological confirmation.

Conclusion:

This case study highlights the importance of utilizing a multidisciplinary approach and imaging modalities, including CT scans , in the diagnosis and management of fibrous dysplasia. Radiological imaging plays a pivotal role in guiding treatment decisions and monitoring disease progression, ultimately contributing to improved patient outcomes.

TO DESCRIBE THE POSTERIOR FOSSA MASS LESION IN A 6 YEAR OLD BOY LIKELY MEDULLOBLASTOMA : A CASE REPORT

Presenting Author: Dr. Shruti Shree
Co- authors: Dr. Suresh Kumar Toppo, Dr. Rajeev Kumar Ranjan.
Affiliations: Department of Radiodiagnosis, RIMS, Ranchi

Introduction:

Medulloblastomas are the second most common malignant brain tumor of childhood, with only high-grade gliomas being more common. They most commonly present as midline masses in the roof of the 4th ventricle with associated mass effect and hydrocephalus.

Case presentation:

This is 6 year old boy presented with complaints of vomiting headache tilting of head towards right since 2 to 3 years of age. On CT scan a heterogeneously hyperdense mass was seen in posterior fossa region resulting in effacement of 4th ventricle and causing obstructive hydrocephalus with periventricular ooze.

On MRI Well defined, T2 & FLAIR mixed signal intense lesion with solid, cystic components and areas of blooming on SWI (hemorrhagic component) noted centered in midline of posterior fossa (from vermis) and seen projecting into 4th ventricle causing mild mass effect on medulla, pons S/0 -? Medulloblastoma with D/D Ependymoma. Moderate obstructive hydrocephalus seen with b/l periventricular CSF seepage.

The boy was operated for obstructive hydrocephalus by placing VP shunt.

Discussion:

Medulloblastoma present as midline masses in the roof of the 4th ventricle with associated mass effect and hydrocephalus. D/d being Ependymoma.

Conclusion:

Treatment typically consists of surgical resection, radiation therapy, and chemotherapy, with the prognosis strongly influenced by surgical resection, the presence of CSF metastases at the time of diagnosis, molecular and histological features and expression of the c-erbB-2 (HER2/neu) oncogene.

TO DESCRIBE THE SUPRASELLAR MASS LESION IN A 5 YEAR OLD BOY RECURRENCE CASE OF CRANIOPHARYNGIOMA

Presenting author: Dr Sunila Kumari singh

Co- authors- Dr Suresh Kumar Toppo, Dr Rajeev Ranjan Affiliations: Department of Radiodiagnosis , Rims, Ranchi

Introduction:

Craniopharyngioma is a benign,often partly cystic sellar/ suprasellar mass that probably arises from epithelial remnants of ratheks pouch.It is the most common nonglial tumour in children. Craniopharyngioma is a slow growing tumour neoplasm with a propensity to recur.

Case presentation:

This is case of 5year old boy presented with complain of headache, vomiting & blurring of vision who has undergone surgery 13 month back for craniopharyngioma.

CT finding shows a well defined complex solid cystic mass lesion in suprasellar region with multiple cystic components showing proteinaceous/hemorrhagic content with solid component showing extensive coarse calcification . VP shunt noted in situ

MRI finding: A well defined lobulated heterogenous lesion noted within the suprasellar region compressing the pituitary inferiorly & also compressing the pituitary stalk, infundibulum & optic chiasma. The lesion appears heterogenously hypointense on T1W , heterogenously hyperintense on T2W/FLAIR images with multiple internal foci of blooming on GRE with partial restriction on DWI/ADC S/O Residual/Relapsing neoplasm.

Discussion:

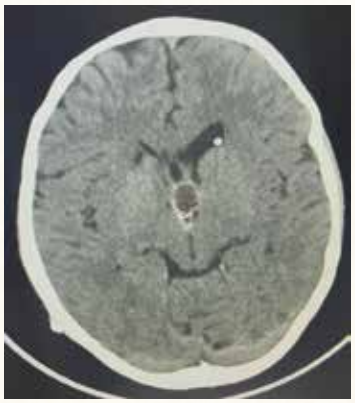

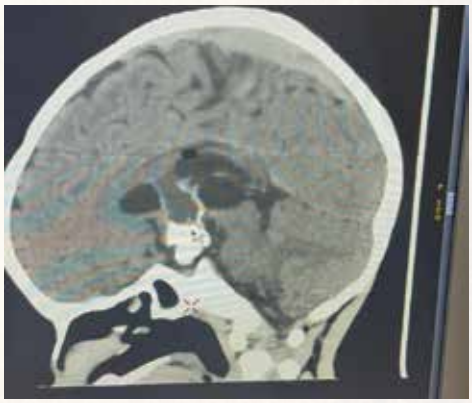

Radiological evaluation, of CT &MRI provide crucial information for diagnosis of Craniopharyngioma. Treatment typically involves a multidisciplinary approach, primary treatment is surgical resection, readiotherapy & hormonal replacement .

Conclusion:

Craniopharyngioma is an uncommon pituitary tumour with high recurrence rate even after surgery. Multidisciplinary Collaboration and long term follow up are essential for optimising patient outcomes and detecting tumour recurrence early.

CAROTID BODY TUMOR - A CASE REPORT

PRESENTED BY Dr Jayanta Kumar Ghosh (Junior Resident 1st year)
Under the guidance of : Dr Suresh Kumar Toppo(Professor and HOD), Dr Rajeev Kumar Ranjan(Associate Professor)
Department of Radiodiagnosis, RIMS, RANCHI

INTRODUCTION :

1. Carotid body tumor also known as carotid body paraganglioma is a highly vascular paraganglioma that arises from the paraganglion cells of the carotid body . Present at the carotid bifurcation with characteristic splaying of ICA and ECA .
2. Most common type of paraganglioma of head and neck.
3. Most commonly seen in 4th to 5th and have female predilection

CASE REPORT :

A 34 year old female presented with paniless swelling in neck on right side which had been slowly growing in size since 1 year .

O/E : Soft , non-tender pulsatile swelling with cystic consistency noted anterior to sternocleidomastoid muscle on right side of the neck which moved side to side but not up or down .

USG findings :

1. Grey scale image - Hypoechoic mass at right carotid artery bifurcation .
2. Hypoechoic mass at the carotid artery bifurcation shows extensive vascularity on color doppler .

CT findings:

1. Contrast CT shows a well defined round to oval rapid enhancing mass lesion in right side of neck at the level of carotid bifurcation with characteristic splaying of Internal Carotid Artery and External Carotid Artery described as Lyre sign .

DISCUSSION :

Carotid body tumor is a extremely vascular paraganglioma . Splaying of internal and external carotid artery helps to differentiate it from other tumors like vagal schwannoma and vagal neurofibroma . It is typically unilateral and b/l in 5 to 10 percent cases . 70 to 80 percent cases are sporadic with small number being familial . It may be associated with MEN II syndrome and Von Hipple Lindau disease . Catecholamine secreting carotid body paraganglioma is rare and may present with paroxysmal hypertension , palpitation , flushing and irritability .

CONCLUSION :

Carotid body tumor is a rare tumor with malignant transformation in 2 to 36 percent of cases showing metastasis to bone, lung and liver . Surgical excision is usually the treatment of choice ,however, the vascular nature makes it challenging. Higher the size, higher are the operative risks.

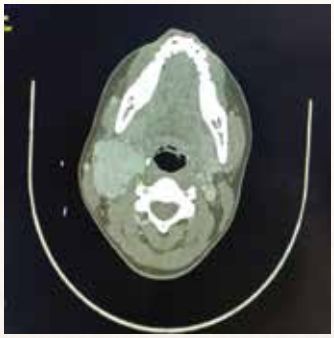

Resona I9

mindray

Diagnostic Ultrasound System

Innovation, in every facet

Infinite imaging solutions

ABD

HiFR STE for liver stiffness quantification

Smart HRI for easy assessment of liver steatosis

Vascular

V Flow for complex hemodynamics evaluation

Precise hardness analysis of carotid wall

Small parts

Smart and accurate breast/thyroid lesion analysis

Complete elastography solution

Cardiology

Auto EF for easy cardiac function evaluation

Quantitative evaluation of myocardial movement

MSK

Elastography for tendon stiffness assessment

CPP for flow analysis of rheumatic arthritis

Urology

Superior image with bi-plane transducer

UWN+ CEUS for prostate cancer diagnosis

23.8" bezel-less full screen

15.6" touchscreen with intuitive interaction

Powered by ZST+

26dB super-silent design

Long-life battery with auto indication

Just fold and go with min 1 meter height

iConsole: intelligent control panel

Full-space floating adjustment

Website : www.mindray.com/in | Toll Free No : 0008-00-85-22-009 | Email : customercare.in@mindray.com

SAMSUNG

Extensive care

We consistently enhance the image quality, improve specialised features, and ergo-dynamics to conduct a wide range of exams from the routine to the complex.
Discover the astounding capabilities of efficient diagnostics and effective care.

Ultrasound	Digital radiography	Point of care solution	IT solution
			
HERA W10 Elite	GM85	HM70 EVO	SonoSync™

T&C apply. Image simulated for representational purposes only.
Cheil-16664/23